A Reappraisal of the Mesozoic/Cenozoic Tectonics and Sedimentary Basins of Peru*

George Devries Klein[1], Fernando J. Zúñiga y Rivero[2], Hugh Hay-Roe[3], and Estuardo Alvarez-Calderon[2]

Search and Discovery Article #10332 (2011)
Posted June 30, 2011

*Manuscript received May 9, 2011, accepted June 6, 2011. Published with permission of the Board of Directors of BPZ Resources, Inc.

[1]SED-STRAT Geoscience Consultants, Inc, 17117 Westheimer Road, PMB #11, Houston, TX, 77082 (gdkgeo@earthlink.net)
[2]BPZ Resources, Inc., 580 West Lake Blvd, Suite 525, Houston, TX, 77079
[3]3126 Royal Crescent, Kingwood, TX, 77379

Abstract

The Mesozoic/Cenozoic tectonics of Peru was controlled by the westward convergence of the continental South American Plate and the northeastern oblique convergence of the oceanic Nazca/Farallon Plate. This tectonic collision developed a composite transform-convergent margin characterized by normal and strike-slip faults that formed extensional/pull apart basins along the western margin of Peru. These extensional/pull-apart basins, such as Talara and Tumbes, are petroliferous and occur both offshore and along Peru's coast.

The coastal basins of Peru show extensive normal, listric, and strike-slip faulting. Immediately to the east of the coastal basins, a belt of Paleozoic low-grade metamorphic and igneous rocks and sediments is known. Onshore, within the northern and central Peruvian Andes**,** a large volcanic gap exists in response to flat-slab subduction during the past 10-7 my.; a classic late Neogene and Quaternary volcanic arc is absent in this northern region, as are paired metamorphic belts.

Moreover, the faulting style of the coastal basins differs from that of classic forearc basins. Instead, the coastal basins of Peru are extensional/pull-apart basins. Trench slope basins occur along the upper wall of the eastern side of the Peru-Chile Trench.

East of this coastal belt of basins are the Andes Mountains which experienced episodic Late Cretaceous and Cenozoic uplift in response to changing rates of plate convergence. Successive orogenic phases developed both fold-and-thrust belts and a series of intermontane and foreland basins.

Three major Cenozoic petroliferous foreland basins occur in the Sub-Andean zone east of the Andes of Peru. These basins, Maranon, Ucayali and Madre de Dios, comprise part of a North- South belt of productive foreland basins occurring from northern Venezuela to Argentina. In Peru, these three foreland basins show regional changes in the age of petroleum systems, with Cretaceous petroleum systems occurring toward

the north (Northern Maranon basin) and Devonian-Permian petroleum systems present in the south (Madre de Dios basin).

These 21 sedimentary basins of Peru showing hydrocarbon potential are organized into four basin fairways representing different tectonic architecture and evolution. From west to east, they are the trench-slope basin fairway, the extensional/pull-apart basin fairway, the intermontane basin fairway, and the foreland basin fairway. These fairways parallel the regional tectonic provinces of Peru and are characterized by their own petroleum systems. The extensional/pull-apart basins and the foreland basins show the greatest potential for future exploration.

The basin styles of Peru define four regional plays and three opportunities for future exploration and production. These include:

- The extensional/wrench system play (Talara, Tumbes and other basins in the extensional/pull-apart fairway),
- An incised valley/shelf edge delta/canyon/fan play (outer continental shelf of Peru),
- An inboard foreland basin play (Camisea, Candamo analogs) associated with a tectonically-driven water drive (Maranon, Ucayali and Madre de Dios basins),
- An outer foreland basin play in the Maranon, Ucayali and Madre de Dios basins associated with a gravity-driven water drive with hydrocarbons trapped by rollover anticlines and faults,
- Attic and by-passed opportunities (Talara basin),
- Re-evaluation of past failures, and
- Re-evaluation of leads proposed by Perupetro, PARSEP, and Gaffney, Cline & Associates.

It is herein predicted that focusing exploration on these plays and opportunities will lead to new major oil and gas discoveries in Peru.

Introduction

The Pacific margin of Peru is an obliquely-convergent plate boundary. It is also a composite transform-convergent margin displaying both strike-slip faults and petroliferous pull-apart basins on the overriding plate (Ryan and Coleman, 1992; Figure 1). These processes characterize the active margin and continental interior of Peru**,** thereby generating numerous opportunities for hydrocarbon exploration particularly within the coastal basins. One can safely predict that some of these exploration ventures will meet with success, as they have in the past.

Past publications dealing with the tectonics of both the active continental margin, onshore Peru, and associated sedimentary basins are characterized by reliable data, some good work, circular reasoning, and *ad hoc* reliance on subduction erosion to explain away the absence of critical features used to define tectonic elements that support existing and standard interpretations applied from other, yet different, regions. Earlier concepts have given way to new insights because of vastly improved seismic acquisition and processing by the oil industry (Zúñiga y Rivero, *et al.,* 1998a, b, c, d, 1999, 2010; Sternbach *et al.,* 2010) and the marine science academic community (Clift *et al.,* 2003**;** Krabbenhoft *et al.,* 2004). An improved regional understanding of the evolution of Peru's sedimentary basins and the entire South American Plate, subjected to the compressive forces of the Pacific Plate and the ridge-push generated along the Mid-Atlantic Ridge by extensional forces, underscores the importance of far-field tectonic influences (Grand, 1994; Ziegler, 1987; Jacques, 2003a, b; Silver *et al.,* 1998) that were previously not understood or considered.

Too often in the past, standard models of active margin tectonics were misapplied to Peru and its active continental margin. These misconceptions were often developed from the use of older seismic reflection data of marginal-quality. New advances in seismic acquisition and processing (Zúñiga y Rivero *et al.,* 1998a, b, c, d, 1999, 2010; Clift *et al.,* 2003; Krabbenhoft *et al.,* 2004; Sternbach *et al.,* 2010) show very different displays that appear to disprove the applicability of many active margin models from other areas. In short, the tectonic evolution of Peru is characterized by its own history that does not necessarily fit entirely other active margin tectonic models, such as those developed from the Japanese Island Arc, the Aleutians, or Indonesia.

This paper reviews both the tectonic elements and evolution of Peru and its petroliferous sedimentary basins, including its offshore region. We integrate events on the overriding South American Plate with those of the subducting Nazca Plate and correlate them to basin-forming processes. Key papers used for this summary and a tectonic correlation diagram are those of Benavides-Cáceres (1999), Mégard (1984), Pardo-Casas and Molnar (1987), Noble *et al.,* (1974), Hampel (2002), Hampel *et al.* (2004), Lonsdale (2005), Silver *et al.* (1998), Pilger (1981, 1984), Ryan and Coleman (1992), Kulm *et al.* (1981), Shepherd and Moberly (1981), Coulbourn (1981), Jacques (2003a, b), Isacks (1988), Jordan *et al.* (1983), Couch *et al.* (1981), Couch and Whitsett (1981), Clift *et al.* (2003), Hickman *et al.* (2005), Sternbach *et al.* (2010), and Zúñiga y Rivero *et al.* (2010), among many others cited herein.

Tectonic Elements

Table 1 summarizes the major tectonic elements of Peru and its offshore regions. Five terms used to describe certain tectonic events or features that were introduced during the past have been renamed (Zúñiga y Rivero *et al.,* 2010; their Table II-2).

Precambrian Continent-wide Lineaments

Northern South America is segmented by four major lineaments (or megashears) that extend into the basement (Shepherd and Moberly, 1981; Jacques, 2003a, b; Figure 2). These megashears separate fundamental zones of plate stress accommodation, which in turn controlled the stratigraphic evolution of, and petroleum systems in, each regional block. The megashears are of Precambrian age and experienced multiple reactivation events since then. They break up the Andean Mountain chain and the South American Plate into several distinct segments, each with its own tectonic history. These megashears control the orientation of major fault systems in the region and represent major zones of crustal weakness that controlled subsequent reactivation (Jacques, 2003a, b).

Four major megashears were identified in Peru. They are, from north to south:

- The Tumbes-Guayana megashear,

- The Huancabamba deflection (also known as the Amazonas megashear), which experienced major reactivation from Late Cretaceous to Eocene (Shepherd and Moberly, 1981; Jacques, 2003a, b),
- The Pisco/Abancay deflection, and
- The Arica deflection**.**

Their relationship to the tectonic elements of the Nazca plate is not fully understood, except that subduction processes along the Peruvian continental margin likely influenced tectonic reactivation along these megashears. In particular, it is most probable that movement along major deep fracture zones on the Nazca plate were propagated onto the South American plate, amplifying reactivation of these megashears (*cf.* Ryan and Coleman, 1992). Far-field tectonic stress induced both by opening of the Atlantic and subduction of the Nazca plate (Silver *et al.,* 1998; Grand, 1994) likely caused reactivation along these megashears also.

Dolores-Guayaquil Megashear

The Dolores-Guayaquil megashear is a major lineament that trends along the bed of the Guayas River in southwest Ecuador and separates accreted Mesozoic oceanic mafic and ophiolitic crust to the west from Precambrian and Paleozoic continental crust to the east (Shepherd and Moberly, 1981; Figure 2). It is characterized by right-lateral movement which formed a pull-apart basin, the Tumbes basin, located in northwest Peru and southwest Ecuador (Zúñiga y Rivero *et al.,* 2010). This megashear has an approximate east-northeast to west-southwest trend. Its southern part displays a partial alignment with the Tumbes-Guiana megashear. However, the Dolores- Guayaquil megashear veers more northerly near the potential intersection of the two. Likely, the Dolores-Guayaquil megashear may have propagated along a zone of weakness developed in association with the Tumbes-Guayana megashear, but is separated from it. The development of the Dolores-Guayaquil megashear may also have been influenced by events as distant as the Caribbean (Jacques, 2003a; Kennan and Pindell, 2009).

The Banco Peru (Peru Bank) occurs on the east side and toward the south end of the Dolores- Guayaquil megashear. Proprietary seismic data suggests it contains a remnant of Talara basin strata and is not related to the accretion of coastal Ecuador to the South American plate (Zúñiga y Rivero, *et al.,* 2010).

Nazca and Farallon Plates

Convergence of the Nazca-Farallon plate was the major oceanic plate tectonic process controlling the Mesozoic and Cenozoic tectonic development of Peru. Originally part of the larger Farallon plate, the Nazca plate formed in response to a process of plate-splitting caused by plate stretching and widespread fracturing (Lonsdale, 2005). This plate-splitting also formed a series of fissure volcanic ridges including the Zavala, Ocola, Alvarado and Sarmiento ridges. The major plate-splitting of the Nazca plate and the Cocos plate immediately to the north occurred along the Galapagos Rift, north of the Carnegie Ridge (Figure 3). That plate-splitting took place during the beginning of Miocene time (23 Ma) and was fully developed by ~19.5 Ma (Lonsdale, 2005; Barckhausen *et al.,* 2008).

Evolution of the Nazca plate is summarized in Figures 3, 4, and 5, showing a series of regional maps redrawn from Lonsdale (2005). A map with reprocessed magnetic anomalies (Figure 3) demonstrates that the Nazca plate split along the Galapagos Rise. NNW-SSE magnetic lineation patterns on the Nazca plate and ENE-WSW magnetic lineations on the Cocos plate, north of the Galapagos Ridge, clearly distinguish the two plates. A reconstruction of the Farallon plate at around 23 Ma, when plate-splitting began (Lonsdale, 2005), is shown in Figure 4 and is based on a restoration of magnetic anomaly data shown in Figure 3. This magnetic anomaly data shows that a large segment of the original Farallon plate is still preserved immediately west of the Peru- Chile Trench (Figure 5), whereas a small segment of it occurs on the eastern edge of the Cocos plate (Lonsdale, 2005).

The Nazca and the remnant Farallon plates are currently converging by a process of flat subduction underneath most of the Peruvian part of the South American plate (Benavides- Cáceres, 1999; Mégard and Philip, 1976; Bump *et al.,* 2008; Kennan, 2000; Figure 6). In fact, the subduction zone along the entire South American Pacific margin is segmented into four regions, of which two are flat-slab subduction zones and two are normal subduction zones (Jordan *et al.,* 1983). In Peru, the flat-slab subduction sector forms a volcanic "gap" on the South American plate. That volcanic gap extends along most of the Peruvian Andes (Kennan, 2000; Hampel, 2002; Figures 6 and 7) and is characterized by a zone of shallow- and intermediate-depth earthquakes located farther inboard from the western edge of the South American plate than areas immediately to the north and south, which are characterized by both steeper subduction and volcanism (Hampel, 2002; Hampel *et al.,* 2004; Figure 7).

The Nazca plate is bounded on the north by the Galapagos Rise, on the west by the East Pacific Rise, on the south by the Juan Fernandez Ridge, and on the east by a small segment of the Farallon plate and the Peru-Chile Trench (Herron, 1972; Lonsdale, 2005). The Galapagos rift is also a spreading center separating the Cocos plate from the Nazca plate, whereas the Juan Fernandez Ridge is both a spreading center and a transform margin. The Nazca Ridge occurs within the plate interior, and its spreading direction is oblique to all its plate boundaries and the direction of convergence.

Ocean Ridges

The Nazca plate contains several ridges and fracture zones.

Nazca Ridge. The Nazca Ridge is more than 1000 km long, 200 km wide, and rises 1.5 km above the ocean floor (Hampel, 2002; Crouch and Whitsett, 1981). It is oriented N42^{o}E, oblique to both the Peru-Chile Trench and the direction of convergence of the Nazca plate, which changed from 90° around 49 Ma to 78° around 11 Ma (Herron, 1972; Pardo-Casas and Molnar, 1987; Lonsdale, 2005). The crustal thickness of the Nazca Ridge is approximately 18 km (Hampel, 2002). It represents the fossil trace of the Easter Island hot spot, which is still active today. The Nazca Ridge has converged obliquely toward the Peru-Chile Trench from the Easter Island hot spot since approximately 50 Ma (Pilger, 1981, 1984; Hampel, 2002; Hampel *et al.,* 2004).

The Nazca Ridge represents a zone of thickened oceanic crust, although of less density than that of the surrounding Nazca plate (Couch and Whitsett, 1981; Figure 8) which buoys up the entire ridge. As the Nazca Ridge crosses the Peru-Chile Trench, the trench floor shallows, shelf terraces are raised and sediment deposition becomes characterized by relatively shallower-water facies (Suess, Von Huene *et al.,* 1988; Resig, 1988, Kulm *et al.,* 1981; Schweller *et al.,* 1981).

The Nazca Ridge converges into, and is being subducted east of, the Peru-Chile Trench at 15°S latitude. Because of its obliquity, the Nazca Ridge has subducted sequentially at different times from a location farther to the north than its present location. The Nazca Ridge initially subducted into the Peru-Chile Trench at 11°S latitude approximately 11.2 Ma (Hampel, 2002; Hampel *et al*, 2004). As ridge subduction continued, its locus of subduction shifted south. Moreover, as the Nazca Ridge crosses the Peru-Chile Trench, the trench floor was uplifted to shallower depths, and then subsided again as the Nazca Ridge was progressively subducted farther south (Resig, 1988; Hampel, 2002; Hampel *et al.,* 2004). Furthermore, the oblique subduction of the Nazca Ridge gave rise to a flat subduction process, underneath Peru, that created a volcanic gap in most of the Peruvian sectors of the South American plate, probably since late Miocene time (11.2 ma; Kennan, 2000; Bump *et al.,* 2008; Mégard and Philip, 1976; Couch and Whitsett, 1981; Hampel, 2002, Hampel *et al.*, 2004, among many others; see also Figure 6).

Carnegie Ridge. The Carnegie Ridge is a prominent aseismic ridge in the northern part of the Nazca plate. This ridge is 1350 km long, up to 300 km wide, and rises 2.0 km above the surrounding sea floor (De la Torre and Macnab, 2005). It formed through the interaction of the Galapagos hot spot and the Cocos-Nazca spreading center, since 23 Ma. Its geometry and crustal thickness are similar to those of the Nazca Ridge (De la Torre and Macnab, 2005).

Other Ridges (Zevallos, Ocola, Sarmiento). These ridges are prominent features on the Nazca plate. The Sarmiento Ridge and probably the Zevallos and Ocola ridges are volcanic ridges fed by fissure eruptions along fracture zones (Lonsdale, 2005). The three ridges are approximately 400 km long and rise from 1 to 2 km above the sea floor.

Fracture Zones

Three major fracture zones, among other smaller ones, are evident on imagery from the Nazca plate. They are the Grijalva, the Viru, and the Mendana fracture zones (Figure 1). They are transform faults and some also are associated with continued fissure eruption during plate movement (Lonsdale, 2005). The Mendana fracture zone may also have formed during plate splitting (Lonsdale, 2005). These fracture zones likely influenced petroleum-trapping mechanisms in Peru, particularly because they are characterized by strike-slip movement within a composite transform-convergent plate boundary displaying oblique convergence (Ryan and Coleman, 1992). Associated strike-slip movement is favored where locking of two plates occurs, such as the shallow-dipping subduction slab east of the Peru-Chile Trench (Hampel, 2002). Such fracture systems and associated fault systems may rupture the entire lithosphere. On land, these strike-slip faults may change along their strike to a braided fault system with subsidiary conjugate and antithetic faults. These faults may appear also as listric faults and flatten at depth (Ryan and Coleman, 1992). A pull-apart basin generally forms in response to the landward extension of these oceanic fracture zones (Ryan and

Coleman, 1992). Opening of these pull-apart basins causes an increase in heat flow (Sawyer *et al.,* 1987) from the transitional crust flooring the basin (Gaffney, Cline & Associates, 2005), and thus favors hydrocarbon maturation.

Satellite imagery (Figure 9) shows a series of fractures on the Nazca plate off the Talara basin. Some of these fracture zones apparently extend and are propagated onto the overriding South American plate. The block fault pattern on the shelf (Figure 9) is similar to mapped fault patterns in the Talara basin (Zúñiga y Rivero et al., 2010).

The Talara basin is classified as an extensional-pull-apart basin because internally its faulted structure shows normal, strike-slip, gravity sliding, and listric faults (Figure 10). It is an excellent example of an oil-productive basin in a composite transform-convergent margin associated with oceanic active fracture zones.

The Mendana fracture zone approaches the Peru-Chile Trench at 10^{o}S at the southern end of the Trujillo and Salaverry basins. Those basins become a potential prospective area if a tectonic and exploration model similar to the Talara basin is applicable there and elsewhere along the Peru margin (Ryan and Coleman, 1992).

Peru-Chile Trench

The Peru-Chile Trench is the submarine expression of the major plate boundary or subduction zone that separates the Nazca (and associated Farallon) and South American plates. It extends from the northwest coast of Colombia to Punta Arenas, Chile (from 5^{o}N to 50^{o}S).

The Peru-Chile Trench reaches a maximum depth of 8065 meters (26,460 ft) below sea level in the Richards Deep off the Chilean margin and is approximately 5900 km (3,666 miles) long. Its mean width is 64 km (40 miles), and it is nearly 590,000 square km in area (228,000 square miles; Schweller *et al.,* 1981; Kulm *et al.,* 1981).

The Peru portion of the trench is, on average, 2 to 3 km shallower than most trenches of the Western Pacific (Schweller *et al.,* 1981). The deepest part of the Peru-Chile Trench off the Peruvian coast is nearly 6 km. The trench axis shoals to a depth of 2 km at its intersection with the Nazca Ridge (Schweller *et al.,* 1981; Hampel, 2002). This shoaling extends beyond the ridge flanks to nearly 200 km north. Convergence and subduction of the Nazca Ridge have increased the slope angle of the continental slope on the overriding plate at their mutual intersection.

The trench slope angle of the incoming Nazca Plate increasingly steepens where the trench axis reaches maximum depths, such as off the Chilean coast. Off Peru, this trench slope ranges between 20° and 30° (Schweller *et al.,* 1981). The width of the Nazca Plate trench slope ranges from 50 to 80 km independent of the depth of the trench axis. The Nazca Plate flexes down along deeper portions of the step-faulted zone, causing the development of horst-and-graben structures.

The continental slope on the South American Plate on the eastern side of the trench is steeper than the trench slope of the Nazca Plate. Slope angles range from 30° to 5° (Schweller *et al.,* 1981). Structural benches were observed on the lower slope and mapped laterally for 10 to 30 km. The internal seismic character of these benches (or terraces) is controversial, with some claiming they are thrust-fault surfaces comprising accretionary prisms at the subduction boundary, or formed by other unknown means (Von Huene *et al.,* 1985; Kulm *et al.,* 1981), whereas others have demonstrated that such an accretionary prism is absent (Hickman *et al.,* 2005; Zúñiga y Rivero *et al.,* 2010).

Subduction Complex and Overriding South American Plate

The subduction complex comprises the contact zone between the Nazca Plate and the toe of the overriding South American Plate, including its lower continental slope. The overriding South American Plate consists of continental crust (Couch and Whitsett, 1981; Couch *et al.,* 1981; Hickman *et al.,* 1985; Zúñiga y Rivero *et al.,* 2010), and its trench wall slopes to the west from 5^{o} to 10^{o} (Schweller *et al.,* 1981).

Until recently, the prevailing paradigm was that the subduction complex of the Peru-Chile Trench was characterized by an accretionary complex of thrust-faulted, off-scraped sediments derived from the subducting Nazca Plate. Essentially, the overriding plate was inferred to function similarly to a bulldozer blade, scraping off sediments from the under-riding oceanic plate. Consequently, these sediments were interpreted to be organized into a series of repeated thrust-faulted stacks of oceanic sediment. The thrust faults in the accretionary complex dip landward and the entire complex comprises the toe of the overriding plate (Von Huene *et al.,* 1985, 1996; Suess, Von Huene, *et al.,* 1988; Kulm *et al.,* 1981; Schweller, 1981; Coulbourn, 1981, among numerous others). The Peru-Chile Trench, therefore, was characterized in the past as displaying a widespread accretionary complex (Von Huene *et al.,* 1985; 1996, Suess, Von Huene *et al.,* 1988; Kulm *et al.,* 1981; Schweller, 1981).

The interpreted existence of these thrust-faulted accretionary complexes came from single- and 24-multichannel seismic records obtained by the oceanographic community during the beginning of the last quarter of the 20th century. Reprocessing has improved line quality somewhat since the late 1980s (Von Huene *et al.,* 1996), but rarely met the quality of industry lines. Moreover, the Deep Sea Drilling Project (DSDP) and its successors, the Ocean Drilling Program (ODP) and the Integrated Ocean Drilling Program (IOPD), made numerous attempts to drill through such subduction complexes to verify the existence of the internal thrust faults. Prior to 1978, both DSDP and ODP recovered material from such thrust faults interpreted to exist within accretionary complexes at only one of 22 sites globally (Coulbourn, 1981). Subsequently, such accretionary complexes and their internal thrust faults were drilled successfully off Barbados, Costa Rica and the Nankai trough off Japan (http://www-odp.tamu.edu/publications/), including ODP Sites 541 and 542 off Barbados (Biju-Duval, Moore, *et al.,* 1984). Thus, drilling confirms that thrust faults exist in these particular accretionary complexes. However, no such confirmation has come from ocean drilling off Peru, where slumped zones were observed instead (Suess, von Huene, *et al.,* 1988).

Sediments recovered from the toe of the overriding South American Plate show evidence of deposition by slumping and debris flows of hemipelagic sediment (Kulm *et al.,* 1981; Coulbourn, 1981). These gravitational sediments build against a backstop of continental crust of the overriding plate (Krabbenhoft *et al.,* 2004). Moreover, industry seismic lines (Ribiana survey of 1993-94; Hickman *et al.,* 2005; Sternbach *et al.,* 2010; Zúñiga y Rivero *et al.,* 1998a, b, c, d, 1999, 2010) show that continental crust extends to the inner (eastern) trench wall of the Peru-Chile Trench, and thrust-faulted accretionary wedges are conspicuous by their absence (Figures 11 and 12). Thus along the subduction complex associated with the Peru-Chile Trench off Peru, evidence for an accretionary prism appears to be, at best, absent (*see also*, Hickman, *et al.,* 2005).

Much of the sediment in the toe of the overriding plate is derived from shelf, slope, and inland sources. The Peruvian continental margin is cut by a series of submarine canyons, including extensive paleocanyons observed in seismic cross-lines obtained in 1993-1994 by the Ribiana survey. Both oceanic and continental sources dispersed sediment into the Peru-Chile Trench preserved as submarine fans, which provide new exploration opportunities (Sternbach *et al.,* 2010).

The lack of an accretionary wedge complex off the Peru margin is explained by a process of subduction erosion. The crust of the Nazca Ridge and the overriding continental South American Plate all break off and are incorporated into the subducting plate as it extends below the overriding plate by underplating. An estimated 800 km of the Nazca Ridge was subducted (Hampel, 2002; Hampel *et al.,* 2004). Estimates of the lateral extent of eroded continental crust range up to 148 km, with erosional rates estimated to range from 3.1 km^3/my. to 13 km^3/my. since 20 Ma (Clift *et al.,* 2003; Clift and Hartley, 2007). Subduction erosion is enhanced where convergence rates exceed 6 ± 0.1 cm/year and where the sediment cover is less than 1 km (Clift and Vannucchi, 2004). Current reported convergence rates at the Peru-Chile Trench are 6.1 ± 1 mm/yr. Thus the survivability of any accretionary complex off Peru, if it existed, likely is in doubt.

Peruvian Portion of the South American Plate

The South American Plate of Peru includes the slope of the east wall of the Peru-Chile Trench, a continental shelf, the Andes Mountains, fold-and-thrust belts, and a series of foreland basins that are known all along the eastern flank of the Andes from Venezuela to Argentina, Cenozoic volcanic rocks and igneous intrusives occurring mainly in both the coastal belt and the Andes (Figure 13), and the Amotape Mountains in the northwest. The Amotape Mountains consist of Precambrian and Paleozoic metamorphosed sedimentary rocks (Figure 13) and represent either an autochthonous horst of intensely deformed Precambrian to Paleozoic rocks or an exotic older terrane accreted along a fossil continental margin (Kennan and Pindell, 2009). In addition, a Precambrian terrane, the Arequipa massif, occurs in southwestern Peru, but because it lacks relevance to petroleum exploration, is not discussed herein.

Shelf and Slope Ridges on South American Plate

Two long and narrow structural ridges were formed on the continental shelf and upper slope during late Cretaceous-early Tertiary time while subduction tectonics on the Peru margin caused associated uplift of the Andes. These two ridges, the Outer Shelf Ridge and the Upper Slope Ridge, parallel the coast and the Andes (Figure 14). Both ridges occur on the South American Plate and are underlain by continental crust.

These two shelf and slope ridges, and associated shorter, transverse shelf uplifts, or local highs, subdivided the Peruvian offshore into a series of Tertiary sedimentary basins (Figure 14). Those Tertiary basins were superimposed on the regional Paleozoic-Mesozoic basins that already existed.

Both longitudinal ridges occur in the subsurface. The Outer Shelf Ridge approximately follows the edge of the continental shelf. However, it is exposed also on the seafloor toward the south near Puerto Caballas At its southern end, the Outer Shelf Ridge merges with the onshore Coastal Cordillera (Figure 14). This merged feature also continues onshore, separating the Mollendo and Moquegua basins for nearly 500 km. Northward, the Outer Shelf Ridge also emerges near Pimentel as the Islands of Lobos de Afuera and farther north at Lobos de Tierra Island (Figure 14) and continues onshore to the north as the Amotape Mountains and into Ecuador. The total length of the Outer Shelf Ridge and its onshore prolongations is approximately 2000 km, of which nearly 900 km represent the submarine structural ridge.

The more westerly submarine ridge, the Upper Slope Ridge, divides the upper trench slope from the middle slope at a water depth ranging from 3000 m. to 4000 m (Figure 14).

Limited early seismic data suggested that both ridges were possible basement features. The 1993 Ribiana seismic survey shows these ridges to consist of Upper Cretaceous to Lower Tertiary, folded strata, buried below Tertiary sediments.

Andes Mountains

With a length of 9000 km, the Andes Mountains are the longest mountain system in the world, reaching a maximum elevation above 7000 m, and a maximum width of 700 km (Kennan, 2000). Its complex geology was described by many workers, including Steinmann (1929), Mégard (1973, 1984), Mégard and Philip (1976), Noble *et al*. (1974), Benavides-Cáceres (1999), Kennan (2000), Bump *et al* (2008), Jordan *et al* (1983), Isacks, 1988), and Miskovic *et al* (2009) among numerous others. This section only highlights the major geological aspects of this mountain system (Figure 13).

The Andean Mountains preserve evidence of three major geodynamic megacycles (Benavides- Cáceres, 1999)**:**

- Precambrian,
- Late Paleozoic to Early Triassic, and
- Late Triassic to the Present

The major tectonic events that caused development of the present-day Andes began during Early Cretaceous, when the South Atlantic started to open (Silver *et al.,* 1998). Three major orogenic intervals are known from the Late Cretaceous to the Present. They were named by Steinmann (1929) as the Peruvian, Incaic, and Quechua orogenies (Table 2). These orogenies are represented by major regional unconformities (Benavides-Cáceres, 1999).

Traditionally, the Andes Mountains in Peru were subdivided into six elements from west to east (Figure 13). These elements are the Coastal Cordillera, the Western Cordillera, the Inter-Andean high plateaus, including the Altiplano in southern Peru, the Eastern Cordillera, a Fold-and-Thrust belt, with three adjacent foreland basins to the east. The Western Cordillera, the Inter-Andean High Plateaus, and the Eastern Cordillera represent subdivisions of the main Andes Mountains.

The Coastal Cordillera. The Coastal Cordillera consists of Precambrian and Paleozoic sedimentary and metamorphic rocks that form part of the Arequipa Precambrian massif, and Mesozoic marine sedimentary rocks. (*cf.* Ramos, 2009; Ministerio de Defensa, 1989, p. 113).

The Western Cordillera. The Western Cordillera is a mountain range that includes the continental divide**;** south of 15° S. it is characterized by an active volcanic arc. It is formed largely by Cenozoic volcanic and intrusive rocks; these volcanics lie on deformed Phanerozoic and even Precambran metamorphics, which are involved in the Peruvian and Incaic fold-and-thrust belts. Along its western flank it is intruded by the Cretaceous Coastal Batholith (Cobbing and Pitcher, 1972; Benavides-Cáceres, 1999) that consists mostly of granitoids.

The Inter-Andean Region. Between the Western and Eastern Cordilleras there is a region of subdued relief and high elevation of around 4000 m.

The Inter-Andean region is traced south to a broad plateau, the Altiplano. Its widest extent coincides with the latitude of the Bolivia orocline, also referred to as the Arica deflection (Isacks, 1988; Jordan *et al.,* 1983). The origin of the Altiplano is attributed to regional crustal shortening and lithospheric thinning associated with a shallow-subducting plate that accommodated differential rates of convergence of the Nazca and South American plates (Isacks, 1988). This shortening was favored by thermally-induced weakness of the overriding plate below the Altiplano (Isacks, 1988). A continuous series of shortening events thickened the crust beneath the Altiplano, causing its widespread uplift. The region is underlain by deformed continental Cenozoic red bed sequences resting on Paleozoic and Mesozoic metamorphic and sedimentary rocks and capped by Upper Tertiary volcanic extrusives (*cf.* Newell, 1949). Immediately to the east of the Inter-Andean region is the well mapped Maranon (or Incaic) fold-and-thrust belt (Mégard, 1973, 1984; Benavides-Cáceres, 1999).

The Eastern Cordillera. West of the High Plateaus is a mountain range with peaks as high as 6000 m and with some glaciated peaks. It consists of Precambrian metamorphics, Lower, Middle and Upper Paleozoic sedimentary units, and several belts of intrusive granitoid bodies, particularly of Permian-Triassic age. Late Permian to Triassic rifting took place along the area of the Eastern Cordillera, with deposition of the clastic nonmarine Mitu Group, which is overlain by the post-rift marine Triassic-Jurassic Pucara Group (Sempere *et al*, 2002). However, in southern Peru, the Mitu Group is overlain by nonmarine fluvial-eolian clastics. Extensive volcanism and emplacement of granitic intrusions accompanied this rifting. Associated lithospheric thinning provided a zone of weakness, but later reactivation occurred during Mesozoic and Cenozoic Andean orogenesis (Sempere *et al.,* 2002).

Maranon Fold-and-Thrust Belt. The Maranon fold-and-thrust belt occurs along the west margin of the Eastern Cordillera (Mégard, 1984). This belt is characterized by gently SW-dipping thrust sheets stacked onto the Pre-Andean basement. Individual thrusts are rooted in Albian calcareous mudstones. The Jurassic Chicama Formation serves as a décollement surface. The fold belt developed during the Incaic orogeny and was reactivated during the Quechua orogeny (Mégard, 1984).

Sub-Andean Fold-and-Thrust Belt. The Sub-Andean fold-and-thrust belt occurs east of the Eastern Cordillera. This fold-and-thrust belt is characterized by a width ranging from 100 to 150 km. It narrows further south near 11° S latitude to 50 km. It is characterized by open folds and thrust faults. The sediments in this fold-and-thrust belt are Mesozoic and Cenozoic, and generally are separated from underlying Paleozoic rocks by a décollement or along a salt layer. Migration of the thrust belt is toward the foreland to the east. Estimates of shortening range from 15 to 30 km (Mégard, 1984) to 84 km (Hermoza *et al.,* 2005; Zúñiga y Rivero *et al.,* 2010) for the Sub- Andean fold-and-thrust belt.

This fold belt flanks four intermontane basins, the Santiago, Bagua, Huallaga and Ene basins (Marocco *et al.,* 1995; Baca-Alvarez, 2004).

Foreland Basins

Immediately to the east of the Sub-Andean fold-and-thrust belt of Peru are three foreland basins, the Maranon, the Ucayali, and the Madre de Dios basins. These three basins are part of a series of foreland basins along the east side of the Andes that extend from Venezuela to Argentina (Mathalone *et al.,* 1995; Jacques, 203a, b; Figure 15). They include many prolific oil-producing basins that derived oil from the La Luna Formation (Cenomanian-Campanian) of Venezuela and its equivalents, such as the Chonta Formation of Peru. Among the most prolific oil-producing basins are the Oriente and Maracaibo basins of Venezuela, the Llanos basin of Colombia, and the Maranon basin of Peru. The Maranon basin also derives a major component of its oil from Paleozoic shales. The three foreland basins, Maranon, Ucayali, and Madre de Dios basins, show a regional change in the age of source-bed distribution with Cretaceous source beds known in the northern Maranon basin and Devonian, Mississippian, and Permian source beds reported from the southern Madre de Dios basin (Figure 16).

Amotape Mountains

The Amotape Mountains consist of deformed Precambrian and Paleozoic sedimentary and metamorphic rocks, forming a horst block along the eastern sides of both the Tumbes and Talara basins. Rocks of Devonian, Mississippian, Pennsylvanian and Permian age were mapped, including the Pennsylvanian Cerro Prieto Formation, which is one of several reservoirs in the Talara basin.

1). Precambrian continent-wide, NNE-SSW Lineaments (through basement)
- **Tumbes-Guyana Megashear**
- **Huancabamba deflection/Amazonas megashear (reactivation – Late K to Eocene?)**
- **Pisco/Abancay deflection**
- **Arica Deflection**

2. Late Megashears – Dolores-Guayaquil megashear (started in Late K – Maastrichtian)

3). Nazca plate
- **a). Ocean Ridges**
  - **Nazca Ridge**
  - **Carnegie Ridge**
  - **Zevallos, Ocola, Alvarado, Sarmiento Ridges**
  - **Inner Ridge (Late K)**
  - **Outer Ridge (Late K)**
- **b). Ocean Fracture Zones**
  - **Grijalva fracture zone**
  - **Mendana fracture zone.**

4). Peru-Chile trench
- **Banco Peru – Subduction Complex (Accretionary Wedge).**
- **Problematic "subduction complexes".**

5). South American plate
- **a). Trench slope**
- **b). Shelf ridges**
  - **Outer Shelf Ridge**
  - **Upper Slope Ridge**
- **c). Andean cordillera.**
  - **Coastal Cordillera – Older – Precambrian to Paleozoic/ Triassic/Jurassic**
  - **Andes Mountains (includes Western Cordillera, Eastern Cordillera Oriental, Altiplano).**
  - **Fold and Thrust Belts – eastern**
- **d). Amotape Mountains**
- **e). Precambrian and Paleozoic accreted terranes**
  - **-Arequipa massif.**

Table 1. Major regional tectonic elements of Peru (from Zúñiga y Rivero et al., 2010).

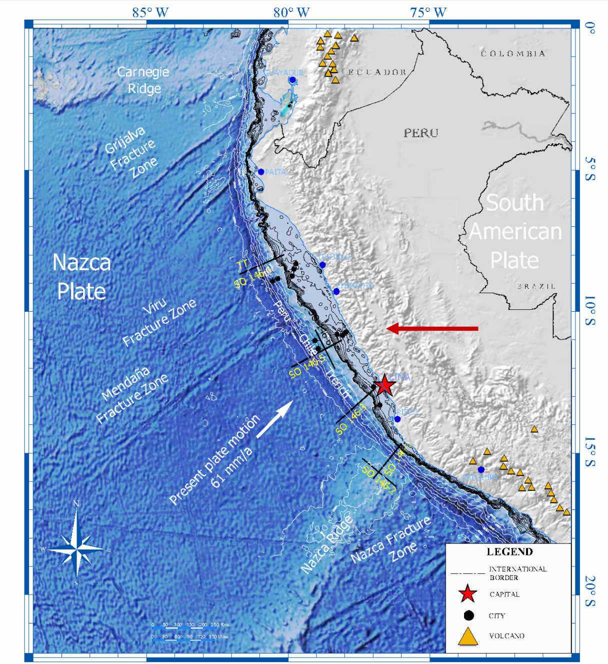

• **Peru margin is excellent example of Composite Transform Margin.**

• **This style of margin controls Peru's tectonic evolution.**

Figure 1. Satellite imagery from Peru Continental margin showing major fracture zones and direction of plate convergence.

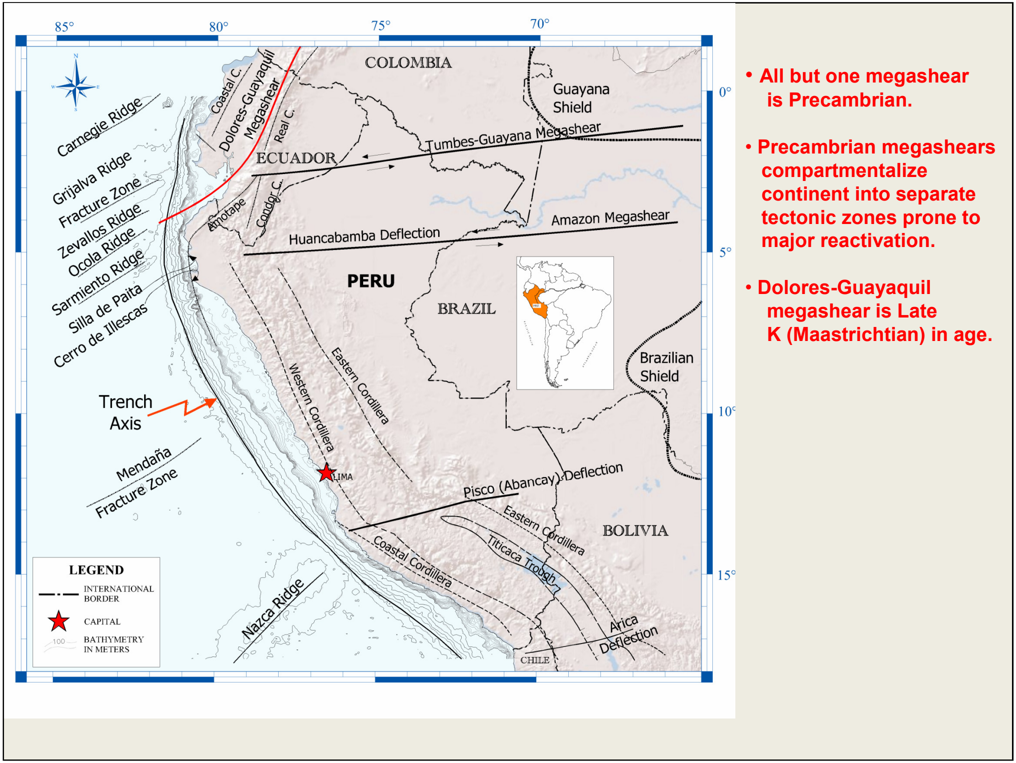

Figure 2. Morphotectonic map of northwestern South America and eastern part of Nazca plate showing major tectonic elements (Redrawn from Shepherd and Moberly, 1981).

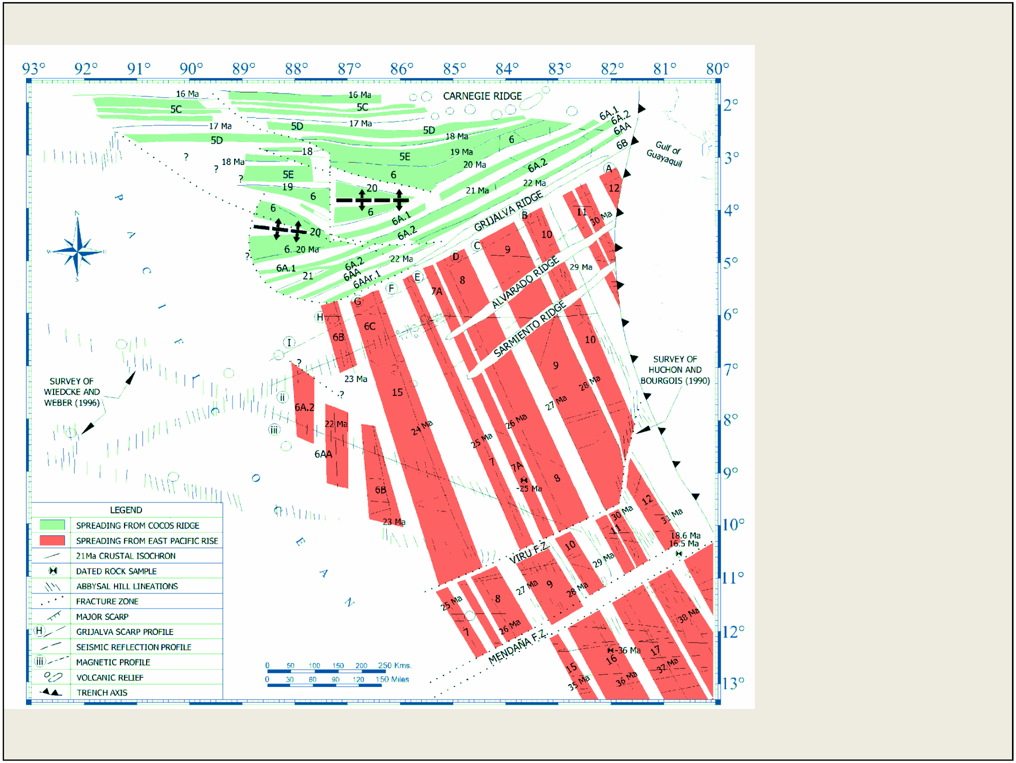

Figure 3. Reinterpreted magnetic anomaly map, East-Central Pacific Ocean (Redrawn from Lonsdale, 2005). Abbreviation: F.Z. – Fault Zone.

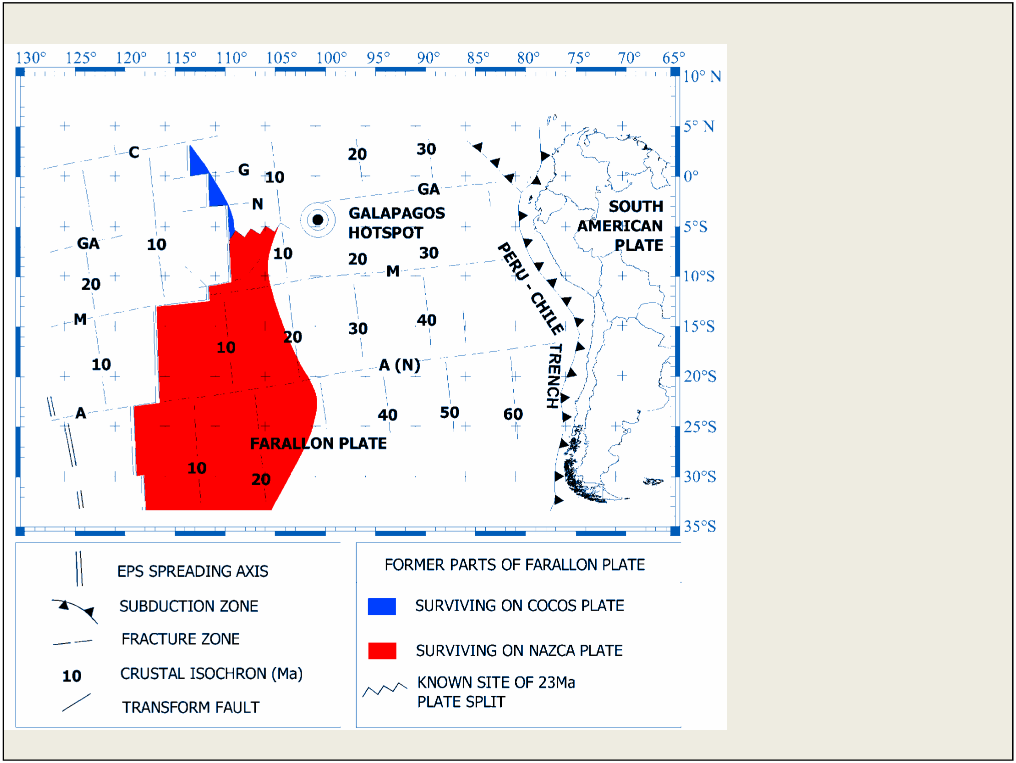

Figure 4. Reconstruction of the geography of Farallon plate, prior to splitting into the Nazca and Cocos plates around 23 Ma (Redrawn from Lonsdale, 2005).

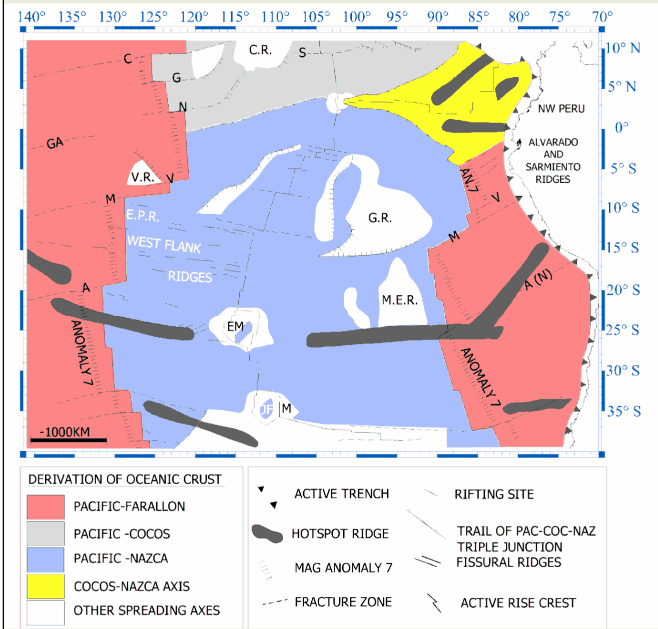

Figure 5. Present-day structural pattern of the east-central Pacific Ocean (Redrawn from Lonsdale, 2005). (*Abbreviations*: MR – Mathematicians ridge, VR –Viru Rise, CR – Clipperton Rise, GR – Galapagos Rise, MER – Mendoza Rise, EM – Easter microplate, M - Mendana fracture zone (East); Marquesas fracture zone (west), C – Clipperton fracture zone, G - Guatemala fracture zone, N – Nicaragua fracture zone, GA – Galapagos fracture zone, V- Viru fracture zone, A (N) – Austral fracture zone (west flank) – Nazca fracture zone (east Flank).

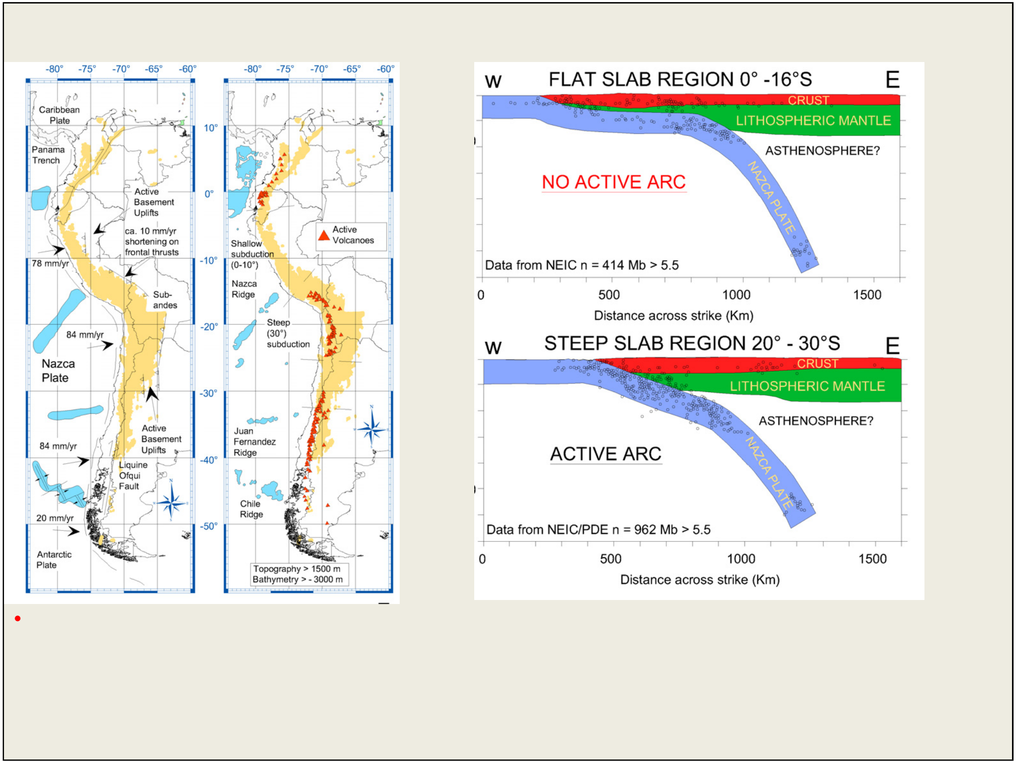

Figure 6. Kinematics of Pacific Plate and Andean Mountains (left) and crustal structure in regions of flat-slab and steep-slab subduction (Redrawn from Bump et al, 2008; Kennan, 2000).

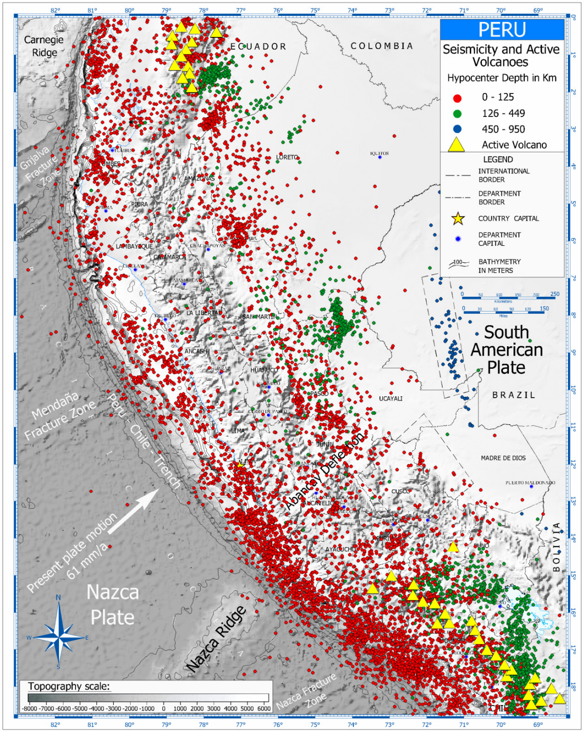

- **Deep earthquakes are inboard along zone of flat subduction.**
- **Flat subduction caused by oblique angle of subducted Nazca Ridge since 11 Ma.**
- **Volcanoes absent in zone of flat subduction.**

Figure 7. Map showing location of Nazca Ridge and spatial distribution of seismicity and active volcanoes, Peru. Earthquake data updated from US Geological Survey National Earthquake Information Center, as of November, 2009 (Redrawn and updated from Hampel, 2002, and Zúñiga y Rivero et al, 2010)

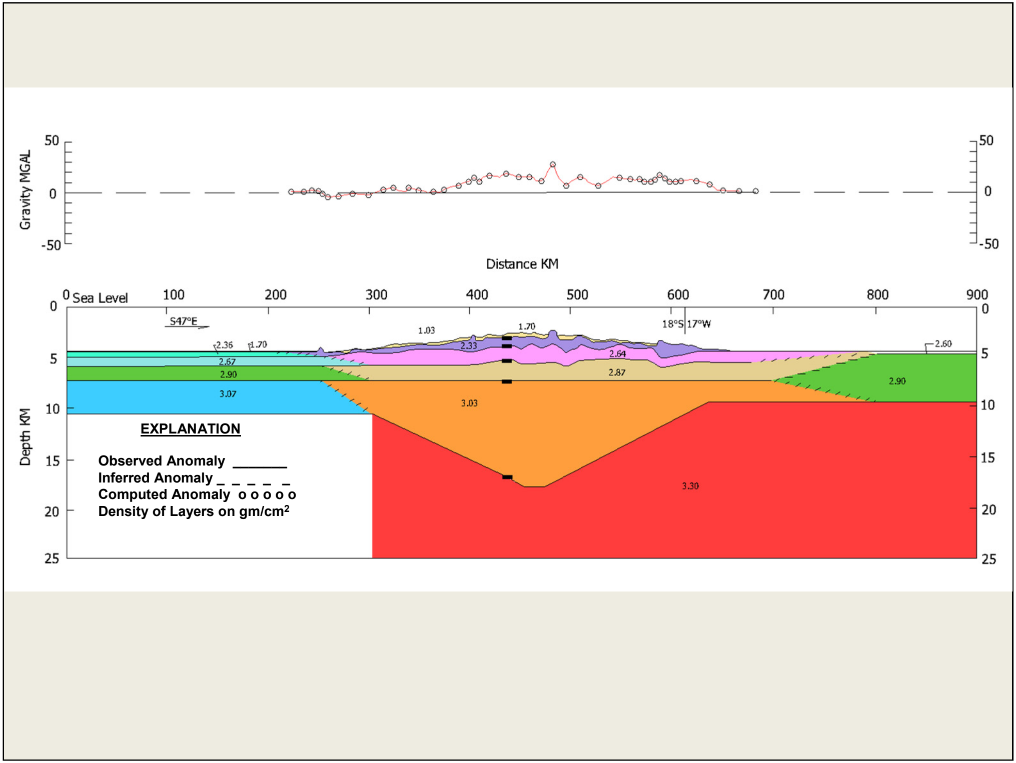

Figure 8. Internal crustal structure of Nazca Ridge with Free-Air gravity anomaly profile. (Redrawn from Couch and Whitsett, 1981).

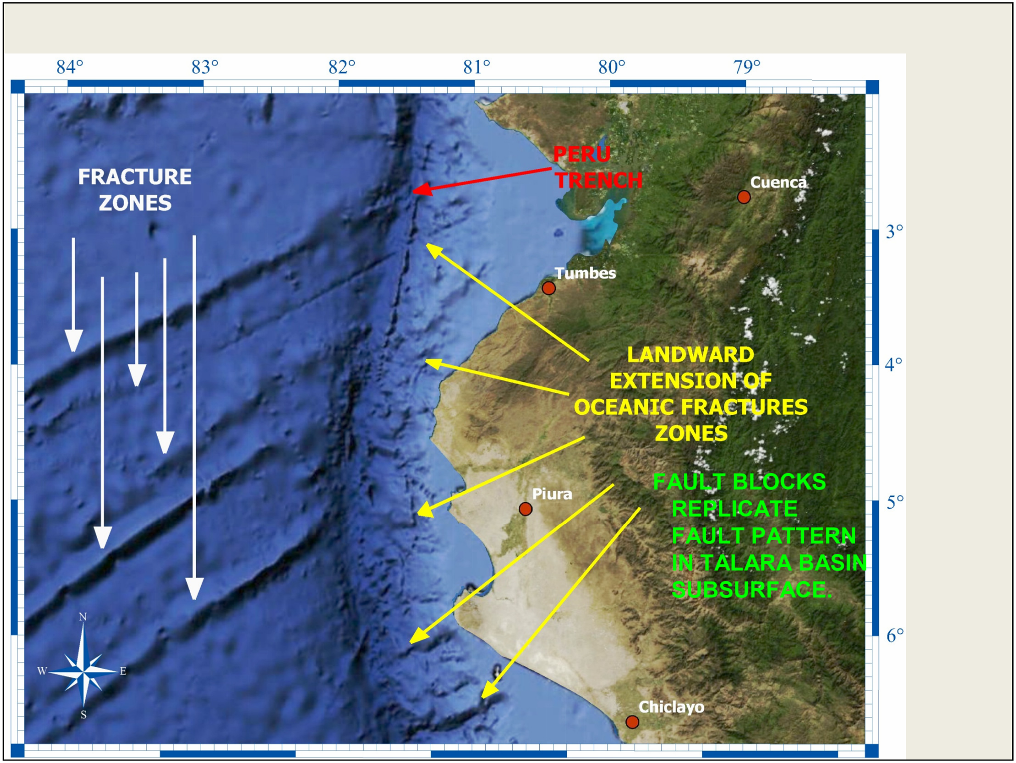

Figure 9. Interpreted Google Earth image of Talara, Peru borderland showing fracture zones and their landward extension. Fault blocks on shelf replicate Talara basin subsurface fault patterns (Redrawn from Zúñiga y Rivero et al, 2010).

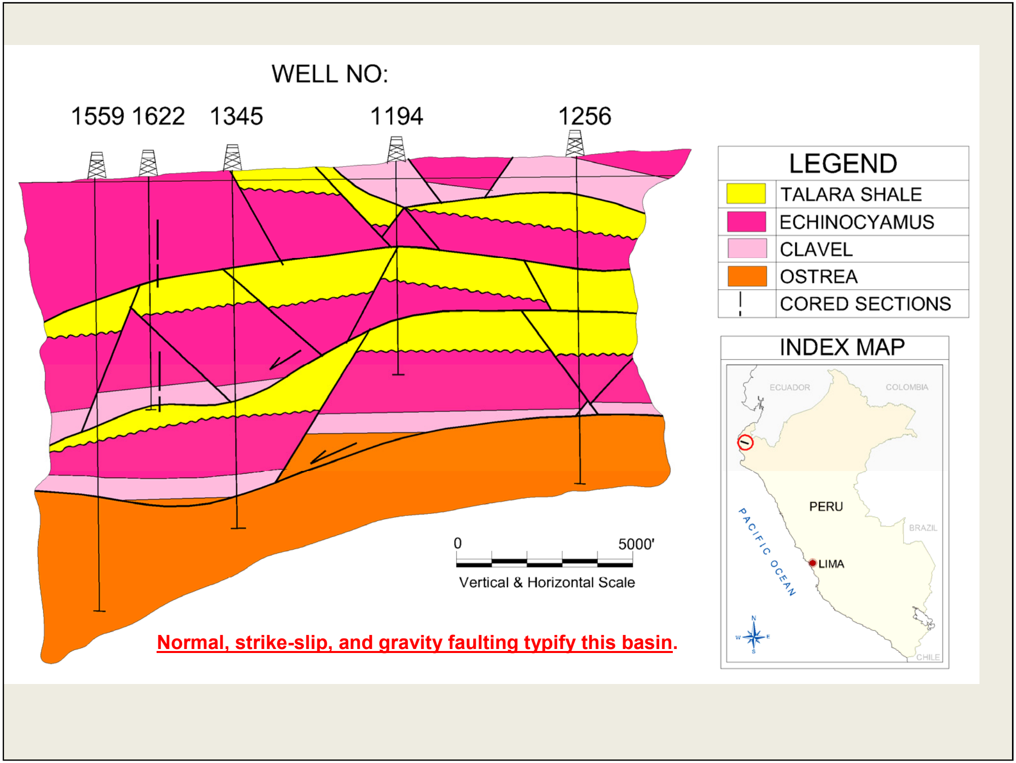

Figure 10. Local cross-section in Talara basin, Perú, showing normal faulting cut by listric gravity slide faults (Redrawn from Zúñiga y Rivero et al, 2010).

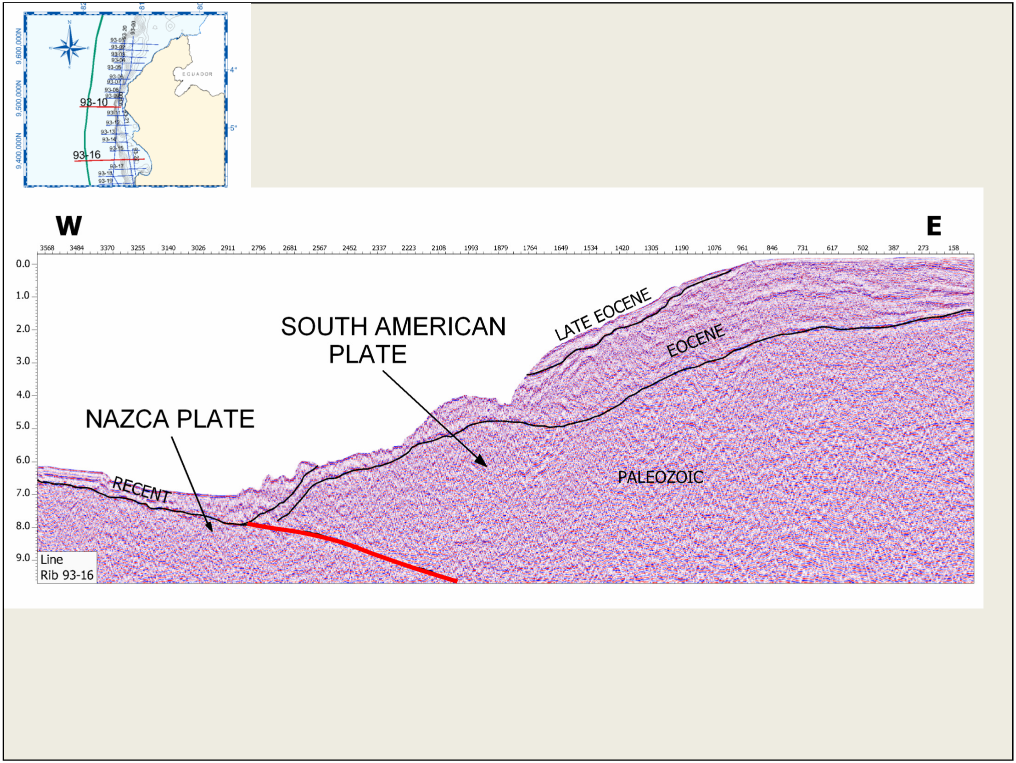

Figure 11. Ribiana seismic line 93-16 Showing lack of accretionary prism, Peru margin. Red line demarcates plate boundaries (Redrawn from Zúñiga y Rivero et al, 2010).

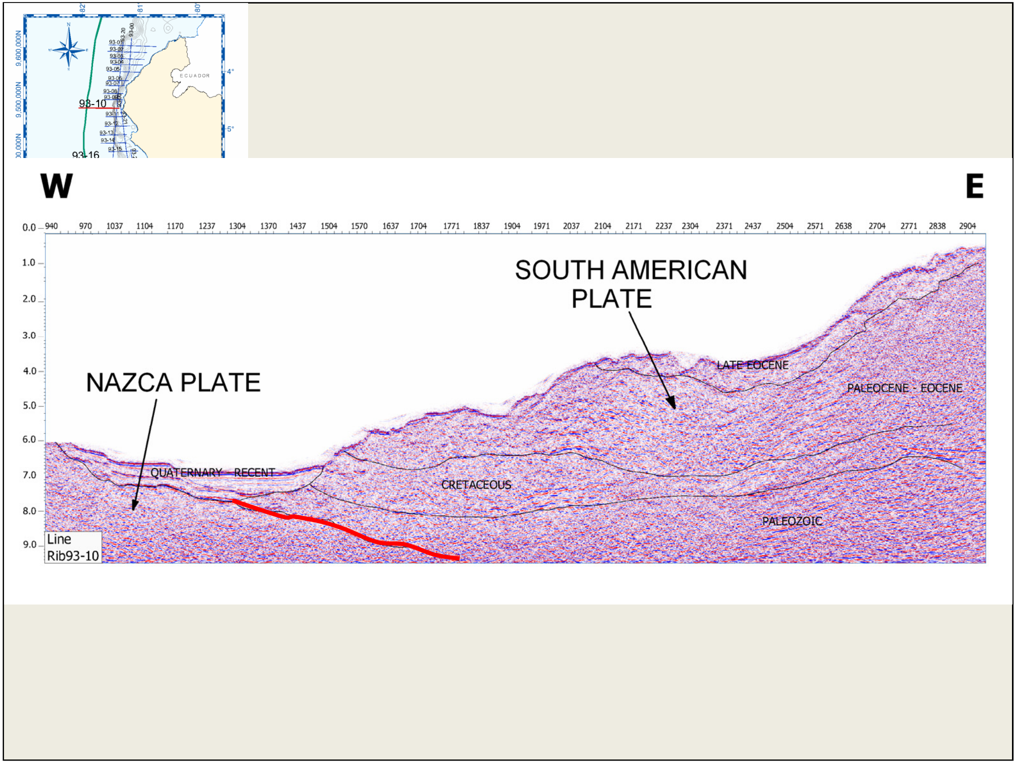

Figure 12. Ribiana seismic line 93-10 Showing lack of accretionary prism, Peru margin. Red line demarcates plate boundaries (Redrawn from Zúñiga y Rivero et al, 2010).

- Maranon FTB occurs on east flanks of Western Cordillera.
- Sub-Andean FTB occurs on east side of Eastern Cordillera.

Figure 13. Morphotectonic units of Peru (Redrawn from Benavides-Caceres, 1999).

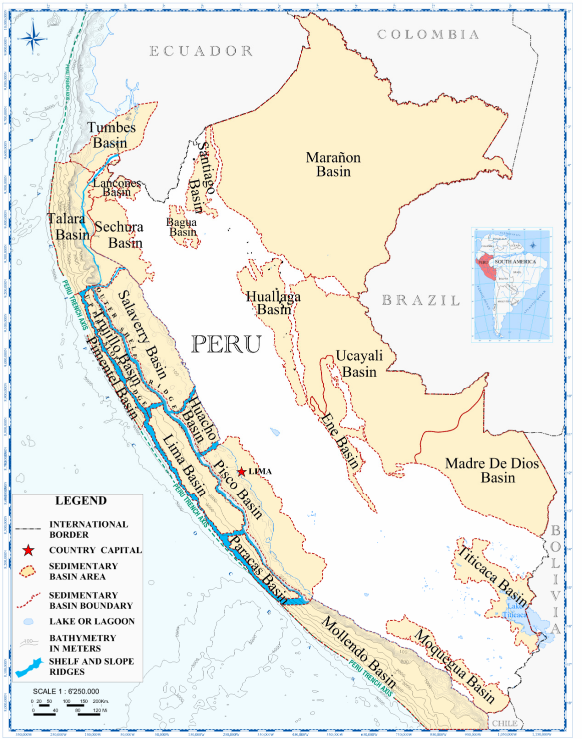

- Outer Shelf and Upper Slope ridges separate the major coastal basins.

Figure 14. Map of Mesozoic/Cenozoic sedimentary basins of Peru and Outer Shelf Ridge and Upper Slope Ridge (Redrawn from Zúñiga y Rivero et al, 2010).

OROGENIC EVENT	GEOCHRONOMETRIC AGE	GEOLOGIC AGE/STAGE
Quechua 4	2.0 – 16. Ma	Late Pliocene to Early Pleistocene
Quechua 3	5 - 4 Ma	Early-Middle Pliocene
Quechua 2	8 - 7 Ma	Upper Miocene (Tortonian)
Quechua 1	20.5 – 12.0 Ma	Early and Middle Miocene (Berdigalian through Serravallian)
Inca 4	22 Ma	Upper Oligocene (Chattian)
Inca 3	30 - 27 Ma	Late Early to Early Late Oligocene (Rupelian and Chattian
Inca 2	43 – 42 Ma	Middle Eocene (Lutetian)
Inca 1	59 – 55 Ma	Late Paleocene to Early Eocene (Thanetian to Ypresian)
Peruvian	84 - 79 Ma.	Late Cretaceous (Santonian to Campanian)
Mochica	100 – 95 Ma	Late Cretaceous (Late Albian to Cenomanian)

Table 2. Geochronological age of major orogenic events, Andes Mountain, Peru (youngest events first) (from Zúñiga y Rivero et al., 2010).

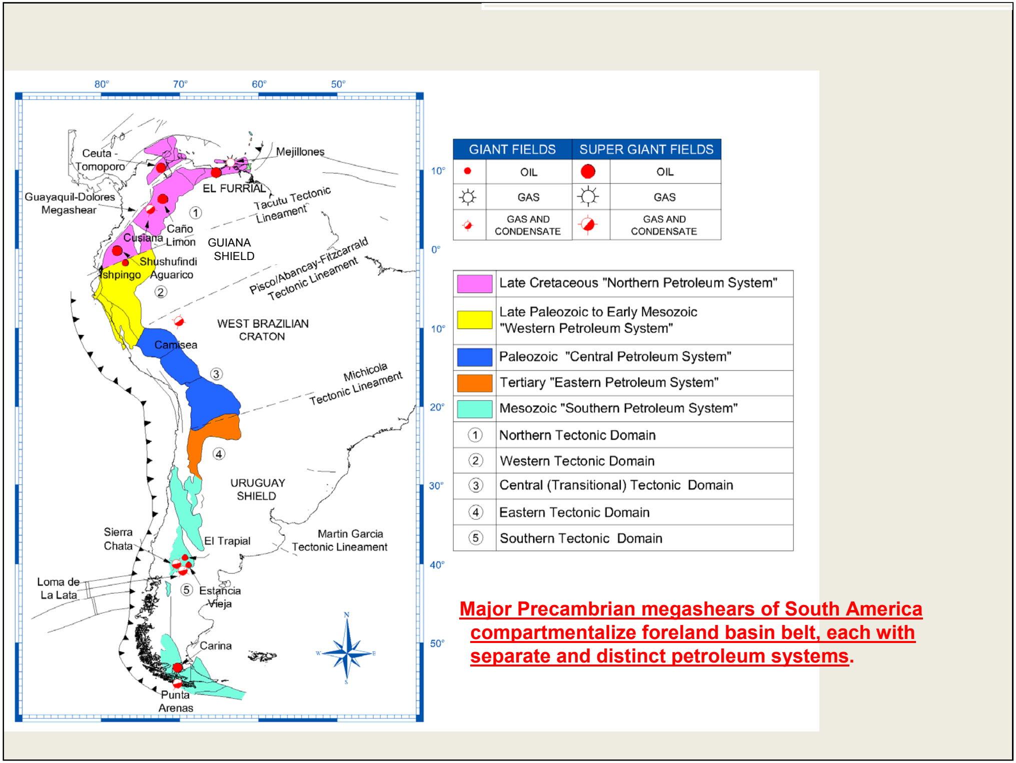

Figure 15. Map of western South America showing distribution of foreland basins east of the Andes Mountains and ages of associated petroleum systems. (Redrawn from Jacques, 2003b)

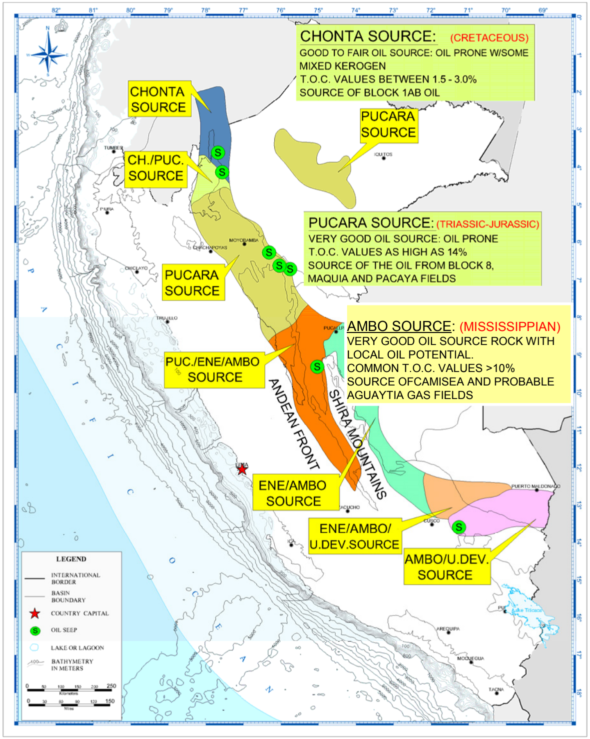

- **Age zonation of petroleum systems occurs on a more local scale as well.**

Figure 16. Generalized map showing distribution and age of source rocks in foreland basins of Peru (Redrawn from Zúñiga y Rivero et al, 2010).

Regional Tectonic Evolution

The Late Mesozoic/Cenozoic tectonic evolution of Peru and its margin is controlled by both the subduction of the Nazca-Farallon Plate system below the South American Plate and regional stresses triggered by the opening of the South Atlantic during late Albian time. The timing of key regional plate tectonic events is summarized in a tectonic correlation diagram (Figure 17).

Much has been written about Andean orogenesis since the first tectonic synthesis by Steinmann (1929). The most recent summary is by Benavides-Cáceres (1999), and the reader is referred to this important paper for a detailed summation. This section only highlights the major regional tectonic events.

A subduction system along the Peruvian continental margin was established at approximately 200 Ma (Shepherd and Moberly, 1981; Pilger, 1981, 1984) following the breakup of Pangea. This early subduction period that lasted during most of the Late Triassic to Cretaceous was dominated by extensional tectonics in most of Peru (Benavides-Cáceres, 1999). In the latest Cretaceous, compression became relevant and the Peruvian, Incaic and Quechua orogenies took place during the Cenozoic.

Compressional tectonics dominated the Peruvian part of the South American Plate when the Farallon Plate became fully active around 70 Ma (Pilger, 1981, 1984). The Farallon Plate broke into the Cocos Plate and the Nazca Plate around 20 Ma by a process of plate splitting (Lonsdale, 2005).

A major driving mechanism for accelerating Andean uplift is the changing rate of plate convergence. Rates of convergence increased on the Farallon and successor Nazca plates between approximately 55 Ma and 42 Ma, and again between 20 Ma and the present day (Pardo- Casas and Molnar, 1987; Figure 17). These periods of increased convergence triggered both the Incaic and Quechua phases of orogeny in the Andes (Figure 17; Table 2).

Convergence rate was very high between 28.3 and 25.1 Ma**,** then dropped to a lower but still a high rate**,** and at about 11 Ma the rate decreased abruptly. Correlations with the compressive events are difficult.

The four orogenic events are shown in Figure 17. The two Cenozoic orogenic events are further subdivided into four shorter episodes as compressional stresses alternated with extensional and inactive regimens. These tectonic episodes were bracketed also by periods of erosion and planation (Kennan, 2000; Mégard *et al.,* 1984; Benavides-Cáceres, 1999). Volcanism is closely associated in time with the Incaic and Quechua orogenic phases (Figure 17).

Summary of Tectonic Events in Peru

Peru has undergone a history of complex tectonism between two major lithospheric plates since the Triassic. That history is summarized in a correlation diagram (Figure 17). Sequentially, these events occurred in the following order:

- Subduction processes began along the Peruvian continental margin at approximately 200 Ma (Shepherd and Moberly, 1981).
- The Mochica orogeny occurred between 100 to 95 Ma (Steinmann, 1929; Mégard, 1984; Benavides-Cáceres, 1999). The timing of that orogeny also coincided in part with the opening of the South Atlantic during the late Albian (Silver *et al.,* 1998).
- The Peruvian orogeny occurred between 84 and 79 Ma (Benavides-Cáceres, 1999). The Peruvian orogeny generated a fold-and-thrust belt along the Western Cordillera (Mégard, 1984; Benavides-Cáceres, 1999).
- Two major events appear to be coeval, the beginning of oceanic spreading of the Farallon Plate nearly 70 Ma (Pilger, 1981, 1984; Lonsdale, 2005), and the initiation of the Dolores- Guayaquil megashear (Shepherd and Moberly, 1981)
- The first of four phases of the Incaic orogeny began at 59 Ma. The Incaic 1 phase ranged from 59 to 55 Ma, the Incaic 2 phase from 43-42 Ma, the Incaic 3 phase from 30 to 27 Ma, and the Incaic 4 phase occurred for a short period around 22 Ma (Mégard *et al.,* 1984; Benavides-Cáceres, 1999; Table 2). Likely, extension or less intense compression occurred between these identified phases. The Maranon fold-and-thrust belt developed in response to the Incaic orogeny, west of the Eastern Cordillera.
- The Nazca Plate, as presently known, split from the Farallon Plate around 23 Ma, and has continued to converge below the Peru-Chile Trench since then (Lonsdale, 2005).
- The rate of plate convergence into the Peru-Chile Trench was episodic, with maximum rates achieved from 44 to 39 Ma and again from 22 to 12 Ma (Pardo-Casas and Molnar, 1987).
- Those episodes of elevated plate convergence coincided with the Inca 2 and both the Quechua 1 and Quechua 2 orogenies.
- The Quechua orogeny also occurred in four phases. Quechua 1 ranged from 20.5 to 12 Ma, Quechua 2 from 8 to 7 Ma, Quechua 3 from 5 to 4 Ma, and Quechua 4 from 2 to 1.6 Ma (Benavides-Cáceres, 1999; Mégard, 1984; Mégard *et al.,* 1984; Table 2).
- The Sub-Andean fold-and-thrust belt formed primarily in response to the Quechua II orogeny along the east side of the Eastern Cordillera.
- The Quechua 2, Quechua 3 and Quechua 4 phases of orogeny have been amplified by the subduction of the Nazca Ridge since 11 Ma (Hampel, 2002; Hampel *et al.,* 2004).
- Episodes of volcanism (Figure 17) are reported to coincide with nearly all phases of the Incaic and Quechua orogenies; they were particularly active in the extensional periods in between the compressive pulses. Two recent episodes starting around 11.3 ma and 7 ma are coeval with subduction of the Nazca Ridge (Noble *et al.,* 1974; McKee and Noble, 1982).
- The orogenic development of the Andes Mountains, particularly during the Quechua orogenic phases, led to development of a series of three foreland basins (Maranon, Ucayali, Madre de Dios) east of the Eastern Cordillera. These basins are part of a South American belt of prolific oil producing basins east of the Andes (Jacques, 2003b).

Petroliferous Sedimentary Basins of Peru

Twenty-one potentially petroliferous sedimentary basins are known both onshore in Peru and the adjacent Peruvian offshore region (Figure 14; Zúñiga y Rivero *et al.,* 1998a, 2010). These basins formed in response to multiple tectonic processes. Seven of these basins are characterized by known hydrocarbon production, whereas others are highly prospective (Perupetro, 2003; Zúñiga y Rivero *et al.,* 1998 a, b, c, d, 1999, 2010).

These 21 Peruvian basins (Figure 14) were formed in response to the combined Late Mesozoic/Cenozoic evolution of the Andean orogenic belt and the active tectonics of the South American Plate margin. Many of these basins are characterized by Precambrian, Paleozoic, and Mesozoic antecedents. Because most of these basins evolved through a complex tectonic history, categorizing them during the past was fraught with difficulty. The basins west of the Peruvian Andes in particular do not appear to fit existing basin classifications (Gaffney Cline & Associates, 2005, their Appendix C; Zúñiga y Rivero *et al.,* 2010).

Several classifications were developed for sedimentary basins, particularly those containing hydrocarbons (Bally and Snelson, 1980; Dickinson, 1974; Klemme, 1975; Kingston *et al.,* 1983a, b; Klein, 1987, 1990; Miall, 1984; Ingersoll, 1988, among others). These basin classifications are rooted in plate tectonics. Distinguishing criteria include the type of plate margin, distance from plate boundary, nature of basement crust, and geodynamic or mechanical/thermal mode of basin formation.

When applying these classifications to the sedimentary basins of Peru (*see* St. John *et al.,* 1984, p.166-167) discrepancies arise between detailed mapping and associated interpretations and basin classification (Tankard, 2002). Peruvian basins generally experienced multiple stages of deformation, inversion, and reactivation during A-subduction (Figure 18).

Many of these basins are characterized by a polyhistory evolving through several cycles of differing basin types. Some of the coastal basins were described as "intermassif" basins (Coulbourn, 1981) to avoid problems associated with applying a classic forearc basin model (*cf.* Tankard, 2002; Gaffney, Cline & Associates, 2005; Hickman *et al.*, 2005; Zúñiga y Rivero *et al.,* 1998a, 2010). Tankard (2002) developed a preliminary model of basin formation utilizing the changing directions of principal stress fields in reference to principal shear zones to explain the evolution of the coastal, intermontane, and foreland basins of Peru.

It is the basins on the west side of the Andes that show the greatest discrepancy with known classifications. Numerous authors (Dickinson and Seeley, 1979; Von Huene *et al.,* 1985; St. John *et al.,* 1984; Bally and Snelson, 1980; Clift *et al.,* 2003; Clift and Hartley, 2007; Fildani *et al.,* 2008) refer to these basins as forearc basins. Forearc basins, however, are commonly associated with B-subduction, such as exemplified by the Japanese island arc (Figure 19; Dickinson and Seeley, 1979, p. 6). Forearc basins are also associated with accretionary prisms and accreted terrains. B-subduction zones are characterized by two colliding, oceanic plates (Figure 19). High seismic velocities comparable to granite off western South America suggest no accretionary prism occurring along the Peru margin. Coulbourn (1981), Marsaglia and Carozzi (1990), Tankard (2002), Gaffney, Cline & Associates (2005), Hickman *et al.*, (2005), and Zúñiga y Rivero *et al* (1998a, 1999, 2010) called attention to factual discrepancies within these basins that fail to fit a forearc model. Moreover, a true volcanic arc inboard from a subduction zone, such as observed in the island arcs of the Western Pacific, is absent in Peru. Instead, areas in Peru where one would expect such arcs consist of Paleozoic slates, quartzites, and low-grade phyllite.

Heat-flow studies in Peru (Henry and Pollack, 1998; Hamza and Muñóz, 1996; Sclater *et al*, 1970; Uyeda and Watanabe, 1982, Yamano and Uyeda, 1990) demonstrated that flat subduction of the Nazca-Farallon plate complex generated low to normal values of heat flow. High heat flow is conspicuous by its absence, particularly in the Andes Mountains of Peru. This finding, along with other evidence, confirms that a typical active margin arc does not exist in Peru at the present time. Thus, the so-called ‘forearc basins’ in western Peru were formed by a different mechanism during at least the past 11 my. and therefore are reclassified herein (Table 3).

Moreover, associated arc massifs in B-subduction zones are commonly floored by glaucophane (or “blue”) schists as well as paired metamorphic belts of glaucophane/greenschist metamorphic facies representing high-temperature/low-pressure zones. Associated amphibolite facies metamorphic zones representing both high-pressure and high-temperature metamorphism also occur in arc massifs (Ernst, 1972, 2008; Miyashiro, 1972). Sporadic reports exist about the occurrence of glaucophane schist in Peru, but no reports of either paired metamorphic belts or amphibolite metamorphic facies in Peru have come to the authors’ attention after an extensive search. Both greenschist and amphibolite metamorphic facies were mapped in Precambrian rocks only (Mégard, 1973), but their distribution appears random. `All Peruvian sedimentary basins, including those west of the Andes (Hickman *et al.,* 2005), are floored by continental crust consisting of granite and Paleozoic metamorphic rocks. They formed in response to the collision of the oceanic Farallon and Nazca plates with the continental South American Plate, and associated tectonic erosion. The overriding continental plate that extends to the eastern wall of the Peru-Chile Trench is eroded by subduction processes (Von Huene *et al.,* 1985; Krabbenhoft *et al.,* 2004; Clift and Hartley, 2007; Clift *et al.,* 2003; Hampel, 2002; Hampel *et al.,* 2004). Both seismic data (Figures 10 and 11) and gravity data (Figure 8) confirm this observation (Couch and Whitsett, 1981; Von Huene *et al.,* 1985; Hampel, 2002; Hampel *et al.,* 2004; Krabbenhoft *et al.,* 2004). Late Mesozoic/Cenozoic accretionary prisms and island arcs are conspicuous by their absence in the Peruvian continental margin (Figures 10 and 11).

Basin Types in Peru

Table 3 summarizes the main criteria used to classify the 21 potentially petroliferous sedimentary basins of Peru (Figure 14). Data used to determine these criteria and basin types include published and released reports by BPZ Energy LLC (2008), BPZ Resources (2010), Perupetro, (2005), PARSEP, (2001a, b, c, d) and numerous other publications and theses (including Baca, 2004; Bump *et al.,* 2009; Portugal, 1974; Myers, 1974; Zúñiga y Rivero *et al.,* 1998a, b, c, d, 1999, 2010). Zúñiga y Rivero *et al* (2010) recently published a detailed summary of each of these basins.

Four types of potentially petroliferous sedimentary basins are recognized in Peru (Table 3). The first is extensional pull-apart basins. These were formed by an initial phase of rifting and associated extension, followed by strike-slip faulting and reorganization of the basins into pull-apart basins. These basins are often associated with propagation of strike-slip faults from subducted regional oceanic fracture zones (*cf.* Ryan and Coleman, 1992; Figure 1). It is now known that the crustal flooring of these extensional pull-apart basins is of sialic, continental origin with heat flow that favored maturation of hydrocarbons. Sedimentary basins that are extensional pull- apart include the Tumbes, Talara, Trujillo, and Salaverry (which is located on the outer shelf), Moquegua, Lancones, and Mollendo basins and are described by PARSEP, (2001c, d), Vega, (2008), and Zúñiga y Rivero *et al.,* (1998, a, b, c, 1999, 2010).

The second type of petroliferous sedimentary basins occurs within Peruvian waters along the east side of the Peru-Chile Trench, where three upper trench slope basins are known. These formed by extension driven by bending of the overriding plate by subduction processes. The upper trench slope basins include the Pimentel, Lima, and Paracas basins (Zúñiga y Rivero *et al.,* 1998a, d, 1999, 2010).

The third type of sedimentary basin is a cluster of intermontane basins within the Andean belt. These basins formed by extension and wrench faulting during a short period between late Oligocene and latest Miocene (7 Ma) time (Marocco, 1995). The five intermontane basins, identified herein, are the Santiago (PARSEP, 2001a), Bagua (Baca-Alvarez, 2004), Huallaga (PARSEP, 2001b), Ene, and Titicaca (Newell, 1949; Sclater *et al.,* 1970) basins.

East of the Andes are three basins that are considered to be polyhistory in origin and represent a fourth type of basin evolution. They are the Maranon, Ucayali, and Madre de Dios basins. Initially formed by Paleozoic rifting, they experienced a cratonic basin phase associated with early thermal subsidence. During Late Cretaceous and Cenozoic time, uplift and loading by the Andes caused these basins to subside as foreland basins. These are classified as Polyhistory: Rift>Cratonic>Foreland basins (Table 3).

Spatial Distribution of the Sedimentary Basins of Peru

The distribution of these 21 sedimentary basins parallels the major tectonic-geomorphic trends of Peru, namely the Peru-Chile Trench and the Andes Mountains (Benavides-Cáceres, 1999). Their distribution defines a series of four basin fairways (Figure 20) grouped according to basin-forming processes. From west to east, these basin fairways (Figure 20) are:

- Trench slope basin fairway,
- Extensional/pull-apart basin fairway,
- Intermontane basin fairway, and
- Foreland basin fairway.

These basin fairways control the potential of future exploration efforts in these areas (*cf.* Jacques, 2003b).

From an exploration standpoint, along composite transform convergent plate boundaries, such as along most of the continental margin of Peru, the role of oceanic fracture zones in developing strike-slip faults, and petroliferous pull-apart basins on the overriding plate (Ryan and Coleman, 1992) present many future hydrocarbon exploration opportunities within the coastal basins of Peru. Regionally, the extensional/pull-apart basins and the foreland basins show the greatest potential for future exploration. It is herein predicted that such accumulations will be found in the future with additional seismic surveys and exploratory drilling.

Future Plays and Opportunities

Our earlier review of the hydrocarbon potential of Peru (Zúñiga y Rivero *et al.,* 2010) shows that it is a country with many unexplored plays and opportunities awaiting drilling. We identified four prospective plays and three additional opportunities (Table 4).

Extensional/Wrench System Play

The underlying rationale for this play is our finding that the continental margin of Peru is a composite transform margin characterized by oblique convergence (*cf.* Ryan and Coleman, 1992). The Talara and Tumbes basins are prime examples of this play (Figure 9). Transfer of stress and orientation of transform fault movements from the Pacific Plate into the South American Plate established a system of normal, gravity and strike-slip faults in both basins (Figure 10). This complex fault system formed hydrocarbon traps, including associated rollover anticlines. Both the Talara and Tumbes basins contain numerous opportunities for exploration, particularly offshore, and include the southern end of the onshore Talara basin. This exploration play characterizes the entire continental shelf of Peru as observed on seismic lines obtained during the 1993 Ribiana survey.

Incised Valley/Shelf Edge Delta/Canyon Fill Play

Cross-lines obtained in 1993-94 by the Ribiana seismic survey show well developed incised valley and submarine canyon fills along the Peruvian continental margin, particularly between latitude 6° S and 15° S. These canyon fills appear to be repeated cyclically containing multiple reservoir opportunities. Moreover, both cross-lines and dip-lines show multiple packages of clinoforms interpreted to represent shelf-edge deltas. Shingled submarine fan opportunities occur downdip from such canyons (*cf.* Sternbach *et al.,* 2010).

The location of the cyclical repetition of these valley/canyon systems and shelf-edge deltas appears to be controlled by faults defining fluvial axes (*cf.* Galloway, 2005). These potential reservoirs in valley/canyon fills and shelf-edge deltas represent another major opportunity in Peru that appears not to have been recognized previously.

Inboard Foreland Basin Play

The inboard foreland basin play is the major oil and natural gas exploration play in South America (Jacques, 2003a, b; Zúñiga y Rivero *et al.,* 2010). Within it are some recently discovered major fields, such as Camisea and Candamo in Peru, and others such as Cusiana in Colombia, and 19 El Furrial in Venezuela, among other fields (Figure 15). In Peru, the inboard regions of the Maranon, Ucayali and Madre de Dios basins are prime candidates for expanded exploration, given past successes, including the Maranon basin fields and the older, Agua Caliente, Aguaytia, and Maquia fields.

Hydrocarbon production in these fields is enhanced by a strong tectonically-derived water drive (*cf.* Garven, 1995). Through heat transfer, heated water enhances maturation and migration of oil from source rocks. This water then aids migration of petroleum into reservoirs. Barson (2002) modeled such a tectonic water drive for the Maranon basin to identify inboard migration pathways into known fields. This modeling should complement seismic surveys in promising areas in future exploration.

The inboard foreland basin play is also associated with the eastern edge of the Sub-Andean fold-and-thrust belt. Trapping mechanisms for hydrocarbons, as exemplified by Camisea (Luquez and Disalvo, 2004), include rollover anticlines on the hanging wall and sealing thrust faults in the footwall.

Outer Foreland Basin Play

This play is distinguished from the inner foreland basin play because of its distance from the flanking thrust belts to the west of the Maranon, Ucayali, and Madre de Dios basins, differences in trapping style, and the presence in some associated fields of heavy, bio-degraded oil (Zúñiga y Rivero *et al.,* 2010). The Tambo, Capahuari, Dorissa, Forestal, San Jacinto, and Shiviyacu fields of the Maranon basin are representatives of this play.

This play appears to be influenced by a gravity-driven water drive from the Andes Mountains following the Quechua orogeny. Recharge areas along the western edge of the three foreland basins established a gravity-flow water drive. As gravity-driven water flows downdip into the deeper portions of the basin, these waters are heated. A process of heat transfer accelerates hydrocarbon maturation. Hydrocarbons migrated toward the eastern, down-basin edges of the Maranon, Ucayali, and Madre de Dios basins and are trapped in local anticlines and along faults. As with the inboard foreland basin play, a hydrogeological model (Barson, 2002) of the Maranon basin during the past 4 my. identified potential pathways leading to known hydrocarbon production. Similar modeling should complement seismic surveys.

Missed Attic Opportunity

The older oil fields of Peru, particularly within the Talara basin, likely contain unknown volumes of by-passed oil. They represent a future exploration opportunity (cf. Daudt et al., 2011). Reservoir formations within the Talara basin that likely contain by-passed oil include the Basal Salina Member of the Salina Formation, the Mogollon Formation, the Parinas Formation, the Helico Formation, the Verdun Formation, and most probably, both Cretaceous formations and fractured Paleozoic quartzites.

Post-Mortem Opportunities from Past Drilling Failures

Early exploration in some of Peru's offshore basins by several companies ended in disappointing results**,** and after drilling two or three wells, the areas were abandoned. Nevertheless, inspection of Figures 21 and *22* from two prospects drilled in the Trujillo basin shows that opportunities were missed by inappropriate well locations by previous operators, partly because they were drilled on Paleozoic basement horsts associated with the Outer Shelf Ridge (Sternbach *et al.,* 2010, Zúñiga y Rivero *et al.,* 2010). A port-mortem re-evaluation of these and other drilling records on file provides new opportunities for successful exploration. Deeper Cretaceous targets and extensive Eocene and Oligocene submarine fans in fault closures and stratigraphic pinchouts appear to define excellent potential prospects (Sternbach *et al.,* 2010).

Re-evaluating Proposed Leads Developed by Perupetro and Associated Contractors

In an effort to stimulate interest from international companies, Perupetro commissioned a variety of consulting reports, both internally (Perupetro, 2005) and by Canadian (PARSEP, 2001, a b, c, d) and US (Gaffney, Cline and Associates, 2005) contractors. Each of these reports proposed promising leads for further exploration. To the writers' knowledge, few to none of these leads have been re-evaluated and drilled. Many of these proposed leads are sufficiently promising that they deserve future evaluation. They represent additional exploration opportunities in Peru.

In summary, with a revised tectonic understanding and a new classification of Peru's 21 petroliferous sedimentary basins, new exploration plays and opportunities have emerged that are worth pursuing.

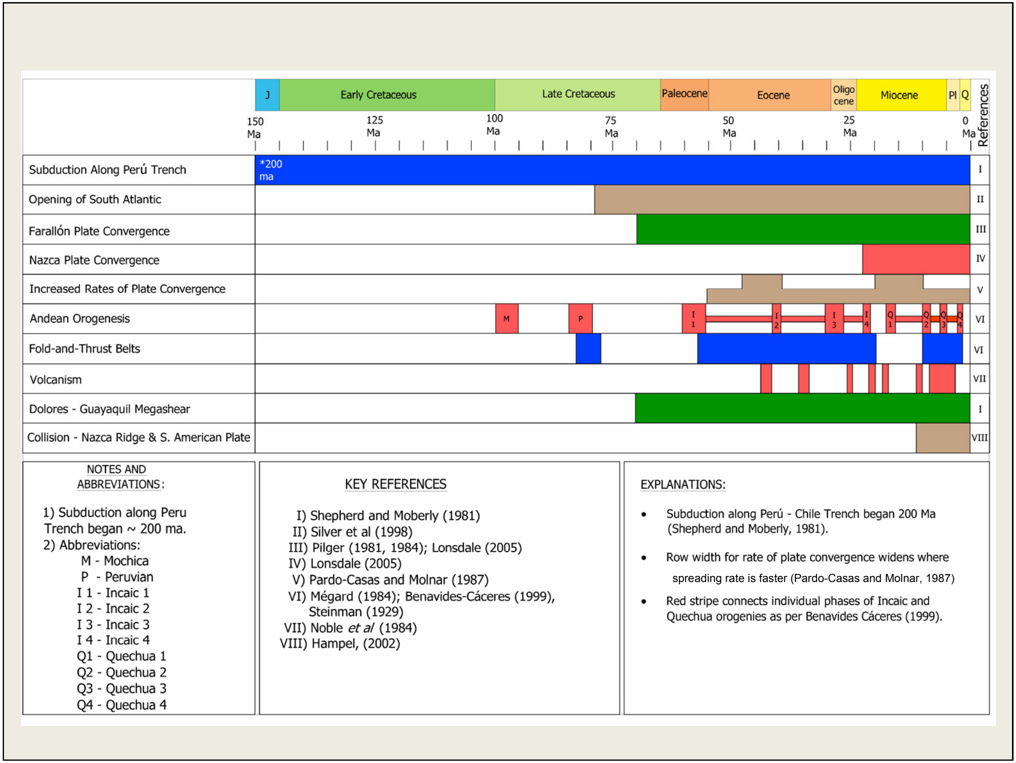

Figure 17. Correlation diagram of major tectonic events on the Nazca Plate and Andes Mountains of Peru (Redrawn from Zúñiga y Rivero et al, 2010).

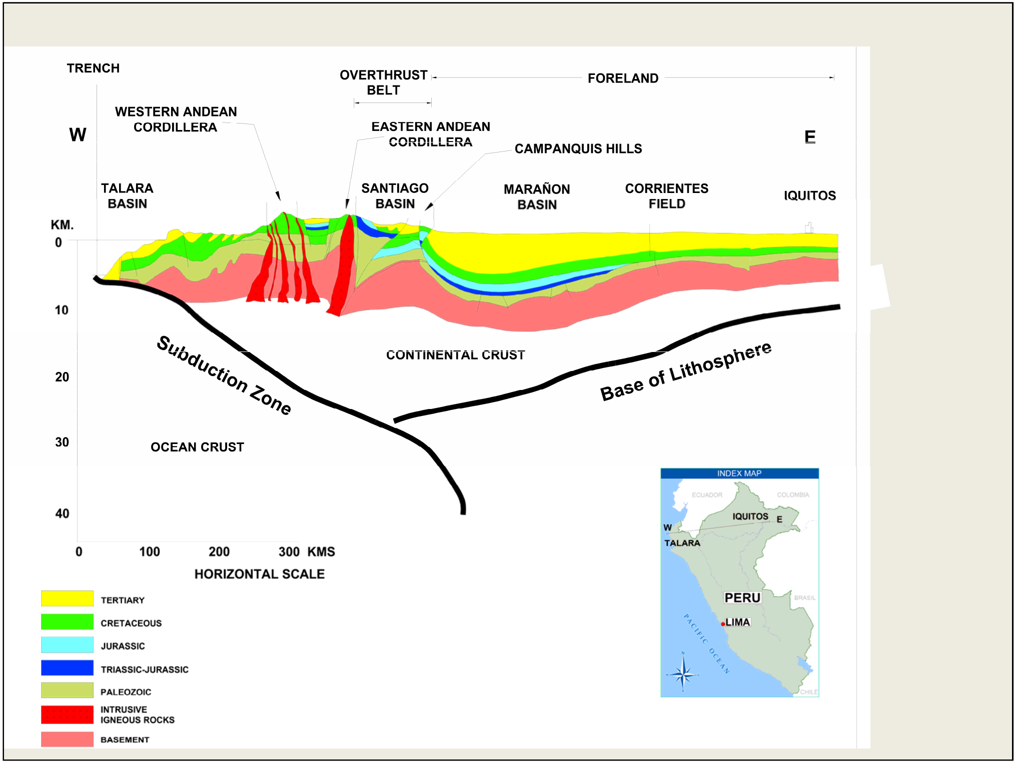

Figure 18. Cross-section displaying typical A-subduction sedimentary basins of Northern Peru (Redrawn from Zúñiga y Rivero et al, 2010).

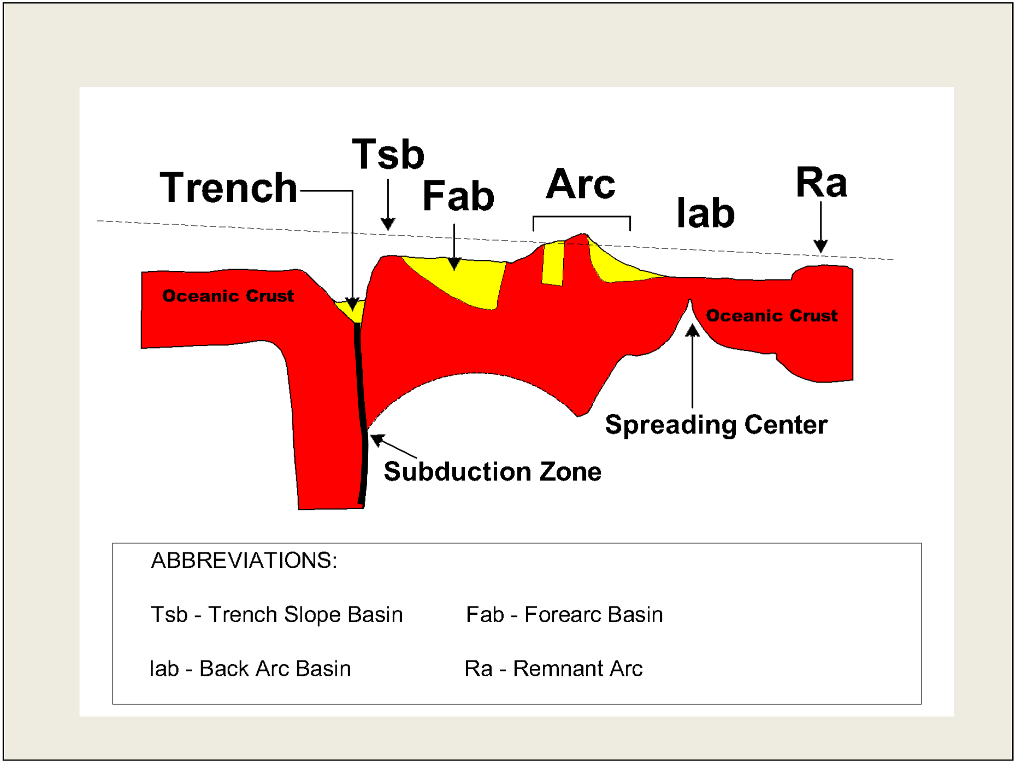

Figure 19. Schematic cross-section of B-subduction sedimentary basins typified by continental margins of Japan, Alaska, and Indonesia. (Redrawn from Southard, 2007).

BASIN	POSITION ON OR WITHIN PLATE	CRUSTAL TYPE	GEODYNAMIC MODEL OF FORMATION	BASIN CLASS OR TYPE
TUMBES	Plate Edge	Continental	Extension and Strike-slip	Extension/Pull-Apart basin
TALARA	Plate Edge	Continental	Rift and Listric fault	Extension/Pull-Apart basin
SECHURA	Plate Edge	Continental	Extension and Strike-slip	Extension/Pull-Apart basin
TRUJILLO	Plate edge	Continental	Extension	Extension/Pull-Apart basin
PIMENTEL	Plate Edge	Continental	Extension	Upper Trench Slope basin
SALAVERRY	Shelf edge	Continental	Extension	Outer Shelf Pull-Apart basin
HUACHO	Shelf edge	Continental	Extension	Outer Shelf Pull-Apart basin
LIMA	Plate Edge	Continental	Extension and Strike-slip	Upper Trench Slope
PISCO	Plate Edge	Continental	Extension and compression	Extension/Pull-Apart basin
PARACAS	Plate Edge	Continental	Extension and compression	Upper Trench Slope basin
MOLLENDO	Plate Edge	Continental	Extension and Strike-slip	Extension/Pull-Apart basin
MOQUEGUA	Inner Plate Edge	Continental	Extension	Extension/Pull-Apart basin
LANCONES	Inner Plate Edge	Continental	Extension and Strike-slip	Extension/Pull-Apart basin
Santiago	Intermontane	Continental	Extension, folding, strike-slip	Intermontane basin
Bagua	Intermontane	Continental	Extension and folding	Intermontane basin
Huallaga	Intermontane	Continental	Extension and folding	Intermontane basin
Ene	Intermontane	Continental	Rifting and strike-slip	Intermontane basin
Titicaca	Intermontane	Continental	Rifting and strike-slip	Intermontane basin
Marañon	Plate interior	Continental	Extension, thermal and loading	Rift>Cratonic>Foreland
Ucayali	Plate interior	Continental	Extension, thermal and loading	Rift>Cratonic>Foreland
Madre de Dios	Plate interior	Continental	Extension, thermal and loading	Rift>Cratonic>Foreland

Table 3. Classification of Cenozoic sedimentary basins of Peru (from Zúñiga y Rivero et al., 2010).

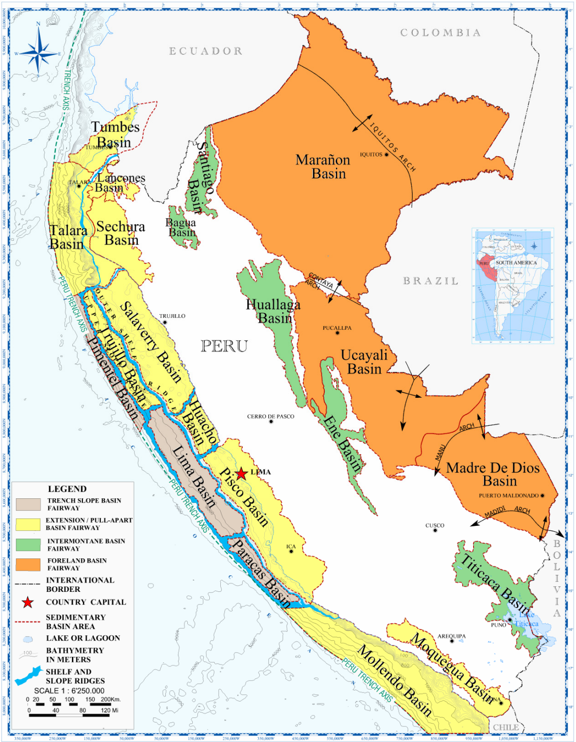

Major tectonic zones of Peru define separate basin fairways characterized by distinct basin forming processes.

Figure 20. Cenozoic sedimentary basin fairways of Peru (Redrawn from Zúñiga y Rivero et al, 2010).

PLAY	**RATIONALE**
Extensional/Wrench System Play.	***Peru Margin is a composite-transform margin characterized by oblique convergence. Traps associated with normal, gravity and strike-slip faults.***
Incised Valley/Shelf Edge Delta/Canyon Fill Play	***Well developed incised valley and submarine canyon fills in Seismic cross-lines (between 6º and 15º S Latitude); Shelf edge delta clinoforms; Shingled submarine fans.***
Inboard Foreland Basin Play.	***Major oil and natural gas exploration play in South America. Hydrocarbon production in play enhanced by a strong tectonic-driven water drive.***
Outer Foreland Basin Play.	***In east side of foreland basins. Play influenced by a gravity-driven water drive from Andes following the Quechua orogeny.***
Missed Attic Opportunity.	***Older fields, especially in Talara basin, likely contain unknown volumes of by-passed oil.***
Post-Mortem Opportunities from Past Drilling Failures.	***Opportunities during past drilling were missed by inappropriate well locations despite presence of DHI's. Re-evaluation presents potential opportunity.***
Re-evaluating Proposed Leads Developed by Perupetro and Associated Contractors.	***Leads and prospects identified by consulting teams to Peru Government during past ten years remain to be drilled.***

Table 4. Future plays and opportunities in Peru.

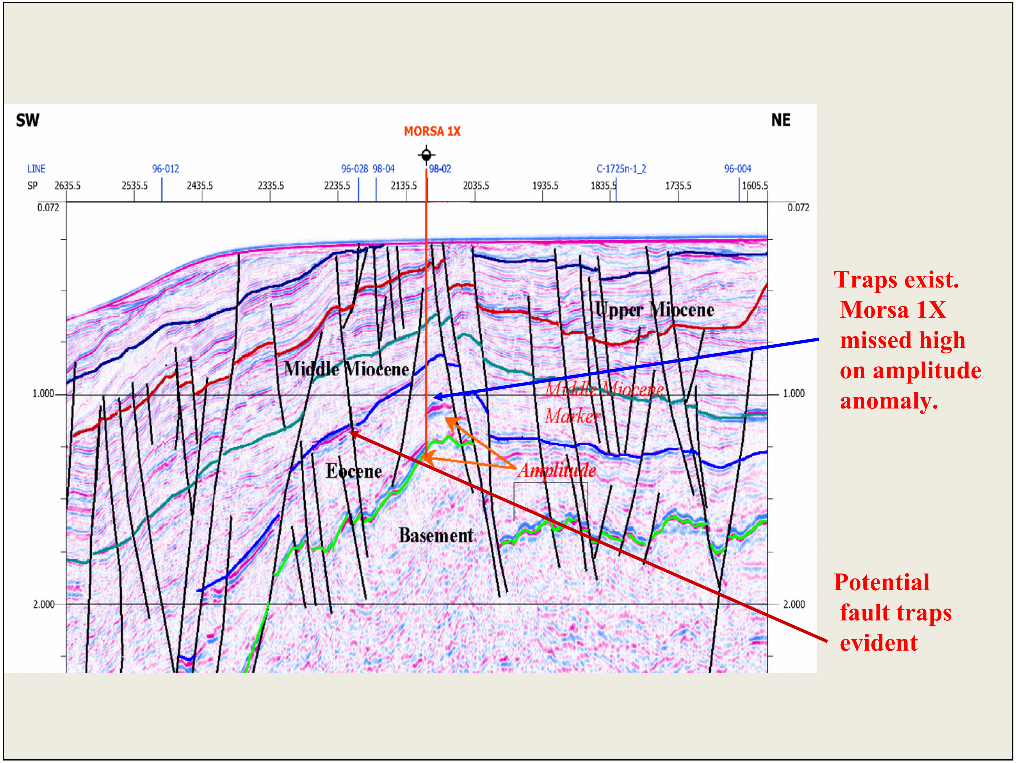

Figure 21. Seismic Line 96-69, conventional display, showing part of four-way dip closure, Morsa Norte 1X well., Trujillo basin (Redrawn from PARSEP, 2001). Morsa 1X well missed high on amplitude anomaly. Alternate opportunities possibly exist on this structural high associated with an amplitude anomaly and numerous fault traps

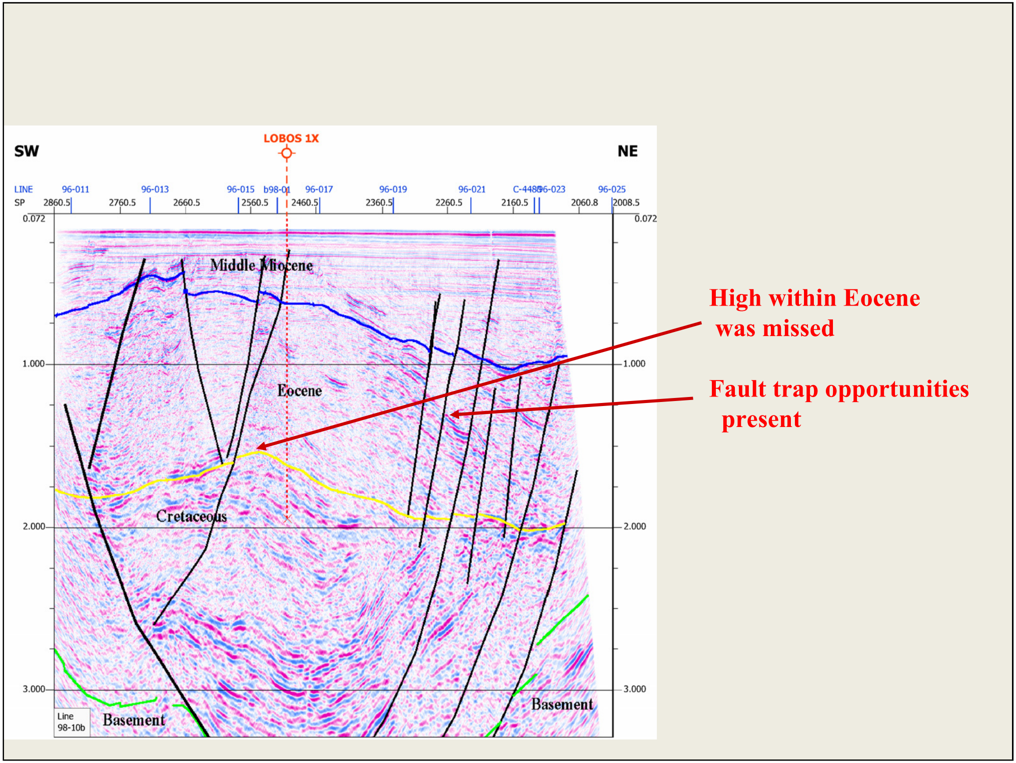

Figure 22. Seismic Line 98-10b, conventional display, at Lobos 1X well., Trujillo basin (Redrawn from PARSEP, 2001). Lobos 1X well missed high within Eocene strata. Several fault traps evident.

Acknowledgments

The authors wish to express their appreciation to Manolo Zúñiga-Pflücker, President and CEO, BPZ Resources, Inc for facilitating this project. Dr. Victor Benavides-Cáceres is thanked for his helpful and cogent review of an earlier version of this manuscript. Kelly Zuniaga-Lopez is thanked for providing outstanding geotechnical support and drafting. Drafting was also completed by Enrique Bravo. Argelia Rozas and Angelica Rozas are thanked for their excellent clerical support.

References Cited

Baca-Alvarez, M., A, 2004, Evolución tectónica y sedimentológica Cenozoica de la Cuenca Bagua (Norte del Peru) y sus implicancias aerodinámicas: Unpublished BS thesis, Universidad Nacional San Antonio Abad Del Cusco: 118p.

Bally, A.W., and S. Snelson, 1980, Realms of subsidence, *in* A.D. Miall, (ed.), Facts and Principles of Petroleum Occurrence: CSPG Memoir 6, p. 9-94.

Barckhausen, U., C.R. Ranero, S.C. Cande, M. Engels, and A. Weinrebe, 2008, Birth of an intraoceanic spreading center: Geology, v. 36, p. 767-700.

Barson, D, 2002, Maranon basin petroleum hydrogeology study: Unpublished Report for Perupetro, 27 p.

Benavides-Cáceres, V., 1999, The Andean cycle, *in* B.J. Skinner, (ed,), Geology and ore deposits of the Central Andes: Society of Economic Geologists Special Publication, v. 7, p. 61-107.

Biju-Duval, B., and J.C. Moore, et al., 1984, Initial Reports of the Deep Sea Drilling Project, v. 78A, U.S. Government Printing Office, Washington, D.C., 621 p.

BPZ Energy, Inc., 2008, Lote XIX- Informe consolidado del segundo period de exploration: Report to Perupetro, 49 p.

BPZ Resources, Inc., 2010, Investor presentation, 16 p.

Bump A., L. Kennan, and J. Fallon, 2008, Structural history of the Andean foreland, Peru, and its relation to subduction zone dynamics: AAPG Search and Discovery article #30062, Web accessed 9 June 2011, http://www.searchanddiscovery.com/documents/2008/08030bump/images/bump.pdf

Clift, P.D., and A.J. Hartley, 2007, Slow rate of subduction erosion and coastal underplating along the Andean margin of Chile and Peru: Geology, v. 35, p. 503-506.

Clift, P.D., and P. Vannucchi, 2004, Controls on tectonic accretion versus erosion in subduction zones: implications for the origin and recycling of the continental crust: Reviews of Geophysics, v. 42, p. 1-31 (Paper No. 2003RG000127).

Clift, P.D., I. Pecher, N. Kukowski, and A. Hampel, 2003, Tectonic erosion of the Peruvian forearc, Lima basin, by subduction and Nazca Ridge collision: Tectonics, v. 22, p.1023.

Cobbing, E.J., and W.S. Pitcher, 1972, The coastal batholith of central Peru: Journal of the Geological Society of London, v. 128, p. 421-460.

Couch, R. and R.M. Whitsett, 1981, Structures of the Nazca Ridge and the continental shelf and slope of southern Peru, *in* L.D. Kulm, et al., (eds.), Nazca Plate: Crustal formation and Andean convergence: GSA Memoir 154, p. 569-586.

Couch, R., R. Whitsett, B. Huehn, and E. Briceño-Guarupe, 1981, Structures of the continental margin of Peru and Chile, *in* L.D. Kulm, et al., (eds.), Nazca Plate: Crustal formation and Andean convergence: GSA Memoir 154, p. 703-726.

Coulbourn, W.T., 1981, Tectonics of the Nazca Plate and the Continental Margin of Western South America, 18° 5 to 23° S, *in* L.D. Kulm, et al., (eds.), Nazca Plate: Crustal Formation and Andean Convergence: GSA Memoir 154, p. 587-6 18.

Daudt, J., J. Rejas, J. Gabriel, J. Galloso, C. Huapaya, and C. Grobav, 2011, Integration of sedimentology and stratigraphy in a 3D static model: example from the *Echinocyamus* Formation in the Block X, Talara Basin, NW Peru: AAPG Search and Discovery article #20099, Web accessed 9 June 2011,
http://www.searchanddiscovery.com/documents/2011/20099daudt/ndx_daudt.pdf

de la Torre, G.M., and R. MacNab, 2005, Carnegie Ridge: a natural prolongation of the Galapagos platform: American Geophysical Union, Fall Meeting, Abstract #T13D-0506.
http://adsabs.harvard.edu/abs/2005AGUFM.T13D0506D

Dickinson, W.R., 1974, Plate tectonics and sedimentation, *in* W.R. Dickinson, (ed.), Tectonics and sedimentation: SEPM Special Publication, v. 12, p. 1-27.

Dickinson, W.R., and D.R. Seeley, 1979, Structure and stratigraphy of forearc regions: AAPG Bulletin, v. 63/1, p. 2-31.

Ernst, W.G., 1972, Occurrence and mineralogic evolution of blue schist belts with time: American Journal of Science, v. 272, p. 657-668.

Ernst, W.G., 2008, Subduction zone metamorphism, calc-alkaline magmatism, and convergent margin crustal evolution: Gondwana Research, v.17.

Fildani, A., A.M. Hessler, and S.A. Graham, 2008, Trench-forearc interactions reflected in the sedimentary fill of Talara basin, northwest Peru: Basin Research, v. 20, p. 305-331.

Garven, G., 1995, Continental-scale ground water flow and geological processes: Annual Review of Earth and Planetary Science, v. 23, p. 89-117.

Gaffney, Cline & Associates, Inc, 2005, Sequence stratigraphic analysis of the Peruvian offshore continental shelf-slope: Unpublished Report to Perupetro, 25 p. with 10 appendices.

Galloway, W.E., 2005, Gulf of Mexico depositional record of Cenozoic North American drainage evolution, *in* M. Blum, S. Marriott, and S. Leclair, (eds.), Fluvial Sedimentology VII: International Association of Sedimentologists, Special Publication v. 35, p. 409-423.

Grand, S.P., 1994, Mantle shear structure beneath the Americas and surrounding oceans: Journal of Geophysical Research, v. 99/B6, p. 11,591-11,621.

Hampel, A., 2002, The migration history of the Nazca Ridge along the Peruvian active margin: a re-evaluation: Earth and Planetary Science Letters, v. 203, p. 665-679.

Hampel, A, N. Kukowski, J. Bialas, C. Heubscher, and R. Heinbockel, 2004, Ridge subduction at an erosive margin: the collision zone of the Nazca Ridge in southern Peru: Journal of Geophysical Research, v. 109/B02101, 19 p.

Hamza, V.M., and M. Muñóz, 1996, Heat flow map of South America: Geothermics, v. 25, p. 599-646.

Henry, S.G., and H.N. Pollack, 1988, Terrestrial heat flow above the Andean subduction zone in Bolivia and Peru: Journal of Geophysics Research, v. 93/B.12, p. 15,153-15,162.

Hermoza, W., W. Brusset, P. Baby, W. Gil, M. Roddaz, N. Guerrero, N., and M. Bolanos, 2005, The Huallaga foreland basin evolution: thrust propagation in a deltaic environment, northern Peruvian Andes: Journal of South American Earth Sciences, v. 19, p. 21-34.

Herron, E.M., 1972, Sea-floor spreading and the Cenozoic history of the East-Central pacific: GSA Bulletin, v. 83, p. 1671-1692.

Hickman, R.G., P.A. Emmet, G.W. Granata, A.F. Cellojon, M. Slot, R.B. Zapana, and Ghazi, T.Y., 2005, New exploration framework and

plays in offshore Peru: AAPG Annual Meeting Abstracts, 2005, Calgary, Alberta, Search and Discovery abstract set #90139, Web accessed 21 June 2011,
http://www.searchanddiscovery.com/abstracts/html/2005/annual/abstracts/hickman.htm

Ingersoll, R.V., 1988, Tectonics of sedimentary basins: GSA Bulletin, v. 100, p. 1704-1719.

Isacks, B.L., 1988, Uplift of the Central Andean Plateau and bending of the Bolivian orocline: Journal of Geophysical Research, v. 93/B4, p. 3211-3231.

Jacques, J.M., 2003a, A tectonostratigraphic synthesis of the Sub-Andean basins: implication for the geotectonic segmentation of the Andean belt: Journal of the Geological Society London, v. 160. P. 687-701.

Jacques, J.M., 2003b, A tectonostratigraphic synthesis of the Sub-Andean basins: inferences on the position of the South American Plate accommodation zones and their control on South Atlantic opening: Journal of the Geological Society, London, v. 160, p. 703-717.

Jordan, T. E., B.L. Isacks, R.W. Allmendinger, J.A. Brewer, V.A. Ramos, and C.L. Ando, 1983, Andean tectonics related to geometry of subducted Nazca Plate, GSA Bulletin, v. 94, p. 341-361.

Kennan, L, 2000, Large-scale geomorphology in the central Andes of Peru and Bolivia: relation to tectonic, magmatic and climatic processes, *in* M. Summerfield, (ed.), Geomorphology and Global Tectonics: Wiley, London, p. 167-192.

Kennan, L., and J. Pindell, 2009, Dextral shear, terrane accretion and basin formation in the northern Andes: best explained by interaction with a Pacific-derived Caribbean Plate, *in* K. James, M.A. Lorente, and J. Pindell, (eds.), The origin and evolution of the Caribbean Plate: Geological Society of London Special Publications, v. 328, p. 487-531.

Kingston, D.R., C.P. Dishroon, and P.A. Williams, 1983a, Global Basin Classification System: AAPG Bulletin, v. 67/12, p. 2175-2193.

Kingston, D.R., C.P. Dishroon, and P.A. Williams, 1983b, Hydrocarbon Plays and Global Basin Classification: AAPG Bulletin, v. 67/12, p. 2194-2198.

Klein, G.D., 1987, Current aspects of basin analysis: Sedimentary Geology, v. 50, p. 95-118.

Klein, G.D., 1990, Maturation-based geodynamic/geochemical classification of sedimentary basins: Sedimentary Geology, v. 69, p. 1-6.

Klemme, H.D., 1975, Giant oil fields in relation to their geologic setting: a possible guide to exploration: Bulletin of Canadian Petroleum Geology, v. 23, p. 30-66.

Krabbenhoft, A., J. Bialas, H. Kopp, N. Kukowski, and C. Hubscher, 2004, Crustal structure of the Peruvian continental margin from wide-angle seismic studies: Geophysical Journal International, v.159, p. 749-764.

Kulm, L.D., J. Dymond, E.J. Dasch, and D.M. Hussong, 1981), Nazca Plate: Crustal formation and Andean convergence: GSA Memoir 154, 824 p.

Lonsdale, P., 2005, Creation of the Cocos and Nazca plates by fission of the Farallon plate: Tectonophysics, v. 404, p. 237-264.

Luquez, J., and A. Disalvo, 2004, Camisea gas fields, Peru: uncertainties and technologies: AAPG International Conference, Cancun, Mexico, Search and Discovery abstract set #90036, Web accessed 21 June 2011, http://www.searchanddiscovery.com/documents/abstracts/2004intl_cancun/extended/A89332.pdf

McKee, E.H., and D.C. Noble, 1982, Miocene volcanism and deformation in the western Cordillera and high plateaus of south-central Peru: GSA Bulletin, v. 93, p. 657-662.

Marocco, R., Boudino, R., and Lavenu, A., 1995, Intermontane Late Paleogene-Neogene basins of the Andes of Ecuador and Peru sedimentological and tectonic characteristics, *in* A.J. Tankard, S. Suarez, and H.J. Welsink, (eds.), Petroleum basins of South America: AAPG Memoir 62, p. 597-614.

Marsaglia, K.M., and A.V. Carozzi, 1990, Depositional environment, sand-provenance and diagenesis of the Basal Salina Formation, lower Eocene, Northwest Peru: Journal of South American Earth Sciences, v. 3, p. 253-267.

Mathalone, J.M.P., and R. Montoya, 1995, Petroleum geology of Sub-Andean basins of Peru, *in* A.J. Tankard, S. Suarez, and H.J. Welsink, (eds.), Petroleum basins of South America: AAPG Memoir 62, p. 423-444.

Mégard, F., 1973, Étude géologique d'une transversal des Andes au niveaeu de Perou Central: Unpub. PhD dissertation, Acadamie de Montpellier: Université des Sciences et Téchniques du Languédoc, 263 p.

Mégard, F., 1984, The Andean Orogenic Period and its major structures in central and northern Peru: Journal of Geological Society, London, v. 141/1984, p. 893-900.

Mégard, F., and H. Philip, 1976, Plio-Quaternary tectono-magmatic zonation and plate tectonics in the central Andes: Earth Planetary Science Letters, v. 33, p. 231-238.

Mégard, F., D.C. Noble, E.H. McKee, and H. Bellon, 1984, Multiple phases of Neogene compressive deformation in the Ayacucho intermontane basin, Andes of central Peru: GSA Bulletin, v. 95, p. 1108-1117.

Miall, A.D., 1984, Principles of sedimentary basin analysis: New York, NY, Springer-Verlag, 490 p.

Ministerio de Defensa/Instituto Geográfico Nacional, 1989, Atlas del Peru, 399 p.

Miskovic, A., R.A., Spikings, D.M. Chew, J. Kosler, A. Ulianov, and U. Schaltegger, 2009, Tectonomagmatic evolution of western Amazonia: geochemical characterization and zircon U-Pb geochronologic constraints from the Peruvian Eastern Cordilleran granitoids: GSA Bulletin, v. 121, p. 1298-1324.

Miyashiro, A., 1972, Metamorphism and related magmatism in plate tectonics: American Journal of Science, v. 272, p. 629-656.

Myers, J.S., 1974, Cretaceous stratigraphy and structure, western Andes of Peru between Latitude 10^{o} and 10^{o}30': AAPG Bulletin, v. 58/3, p. 474-487.

Newell, N. D., 1949, Geology of the Lake Titicaca region, Peru and Bolivia: GSA Memoir 36, 111 p.

Noble, D.C., E.H. McKee, E. Farrar, and U. Petersen, 1974, Episodic Cenozoic volcanism and tectonism in the Andes of Peru: Earth and Planetary Science Letters, v. 2, p. 213-220.

Pardo Casas, F., and P. Molnar, 1987, Relative motion of the Nazca (Farallon) and South American Plates since Late Cretaceous time: Tectonics, v. 6, p. 233-248.

PARSEP, 2001a, Final Report on the Santiago basin, v. 1: Internal Report to Perupetro, 110 p.

PARSEP, 2001b, The Huallaga basin and adjacent area: Internal Report to Perupetro, 67 p.

PARSEP, 2001c, The remaining undiscovered hydrocarbon potential of the Trujillo offshore basin, v. 1: Internal Report to Perupetro, 109 p.

PARSEP, 2001d, Hydrocarbon potential of the Salaverry offshore basin, Peru: Internal Report to Perupetro, 41 p.

Perupetro, 2003, A renewed exploration opportunity (revised edition): Perupetro SA, Lima, Peru, 41p.

Perupetro S.A. 2005, Oil Prospectivity in the Salaverry Basin. Part of a regional Project funded by the USTDA and conducted for Perupetro by

Gaffney, Cline &Associates & Perupetro S.A.

Pilger, R. H., Jr., 1981, Plate reconstructions, aseismic ridges, and low-angle subduction beneath the Andes: GSA Bulletin, v. 92, p. 448-456.

Pilger, R.H., Jr., 1984, Cenozoic plate kinematics, subduction, and magmatism-South American Andes: Journal of the Geological Society of London, v. 141, p. 793-802.

Portugal, J.A., 1974, Mesozoic and Cenozoic stratigraphy and tectonic events of Puno-Santa Lucia area, Dept. of Puno, Peru: AAPG Bulletin, v. 58/6, p. 982-999.

Ramos, V.A., 2009, Anatomy and global context of the Andes: main geologic features and the Andean orogenic cycle, *in* S.M. Kay, V.A. Ramos, and W.R. Dickinson, (eds.), Backbone of the Americas: Shallow subduction, plateau uplift, and ridge and terrane collision: GSA Memoir 204, p. 31-66.

Resig, J., 1990, Benthic forminiferal stratigraphy and paleoenvironments off Peru, *in* E. Suess, R. von Huene, et al., (eds.), 1988 Proceedings Leg 112, Ocean Drilling Program Scientific Research, v. 112, p. 263-282.

Ryan, H. F., and P.J. Coleman, 1992, Composite transform-convergent plate boundaries: description and discussion: Marine and Petroleum Geology, v. 9, p. 89-97.

Sawyer, D.S., A.T. Hsui, and M.N. Toksoz, 1987, Extension, subsidence and thermal evolution of the Los Angeles basin–a two dimensional model: Tectonophysics, v. 133, p. 15-32.

Schweller, W.J., L.D. Kulm, and R.A. Prince, 1981, Tectonics, structure and sedimentary framework of the Peru-Chile trench, *in* L.D. Kulm, et al., (eds.), Nazca Plate: Crustal formation and Andean convergence: GSA Memoir 154, p. 323-349.

Sclater, J. G. V. Vacquier, and J.H. Rohrhirsch, 1970, Terrestrial Heat flow measurements on Lake Titicaca, Peru: Earth and Planetary Science Letters, v. 8, p.45-54.

Sempére, T., G. Carlier, P. Soler, M. Fornari, V. Carlotto, J. Jacay, A. Arispe, D. Nerandeau, J. Cardenas, S. Rosas, and N. Jimenez, 2002, Late Permian – Middle Jurassic lithospheric thinning in Peru and Bolivia, and its bearing on Andean-age tectonics: Tectonophysics, v. 345, p. 153-181.

Shepherd, G. L., and R. Moberly, l98l, Coastal Structure of the Continental Margin, Northwest Peru and Southwest Ecuador, *in* L.D. Kulm, J. Dymond, E.J. Dasch, and D.M. Hussong, (eds.), Nazca Plate-Crustal Formation and Andean Convergence: GSA Memoir 154, p. 351-391.

Silver, P.G., R.M. Russo, and C. Lithgow-Bertelloni, 1998, Coupling of South American and African plate motion and plate deformation: Science, v. 297, p. 60-63.

Southard, J.B., 2007, Lecture Notes, 12.110 Sedimentary Geology, Chapter 11: M.I.T. Dept. of Earth, Atmospheric and Planetary Sciences: http://ocw.mit.edu/courses/earth-atmospheric-and-planetary-sciences/12-110-sedimentary-geology-spring-2007/lecture-notes/ch11.pdf

St. John, B., A.W. Bally, and H.D. Klemme, 1984, Sedimentary provinces of the world – hydrocarbon productive and non-productive: AAPG Explanation to accompany map, 35 p.

Steinmann, G., 1929, Geologie von Peru: Heidelberg, KarlWinter, 448 p.

Sternbach, L.R., S. Bang, C. Biachi, J. Cespedes, Y. Han, and D.S. Choi, 2010, Offshore Peru, Trujillo basin, Block, Z-46: 2D PSTM Seismic processing reveals deep basins, normal and transtensional faulting and thick Eocene/Oligocene stratigraphic complex submarine fans linked to evidence of Hydrocarbons/DHI's: AAPG Search and Discovery Article #10263, Web accessed 20 June 2011, http://www.searchanddiscovery.com/documents/2010/10263sternbach/images/sternbach.pdf

Suess, E., R. von Huene, et al., 1988, Proc. ODP, Initial Reports, 112: College Station, TX (Ocean Drilling Program). Web accessed 20 June 2011.
http://www-odp.tamu.edu/publications/citations/cite112.html

Tankard A. J., 2002, Tectonic framework of basin evolution in Peru: Report to PARSEP, 23 p.

Uyeda, S., and T. Watanabe, 1970, Preliminary report of terrestrial heat flow study in the South American continent; distribution of geothermal gradients: Tectonophysics, v. 10, p. 235-242.

Uyeda, S., and T. Watanabe, 1982, Terrestrial heat flow in western South America; Tectonophysics, v. 83, p. 63-70.

Vega, M., 2008, Modelo tectono-sedimentario del prisma de acreción para el antearco del norte del Peru: Nuevas orientaciones para la exploración: VI INGEPET EXPRO4-MV026, PowerPoint presentation, 16 slides.

Von Huene, R., L.D. Kulm, and J. Miller, 1985, Structure of the Frontal Part of the Andean Convergent Margin: Journal of Geophysical Research, v. 90/B7, p. 5429-5442.

Von Huene, R., I.A. Pecher, and M.A. Gutscher, 1996, Development of the accretionary prism along Peru and material flux after subduction of

Nazca ridge: Tectonics, v. 15, p. 19-33.

Yamano, M, and S. Uyeda, 1990, Heat-flow Studies in the Peru Trench Subduction Zone, *in* E. Suess, R. von Huene, et al., Proc. ODP, Scientific Results, v. 112, p. 653-661.

Ziegler, P.A., 1987, Late Cretaceous and Cenozoic intraplate compressional deformations in the Alpine foreland–a geodynamic model: Tectonophysics, v. 137, p. 389-420.

Zúñiga y Rivero, F.J, J.A. Keeling, and H. Hay-Roe, 1998a, Attractive potential seen in 10 subbasins offshore Peru: Oil and Gas Journal, v. 96/36, p. 117-122.

Zúñiga y Rivero, F.J, J.A. Keeling, and H. Hay-Roe, 1998b, Peru onshore to deepwater basins should have large potential: Oil and Gas Journal, v. 96/42, p. 88-95.

Zúñiga y Rivero, F.J., J.A. Keeling, and H. Hay-Roe, 1998c, Oil and gas potential in offshore waters: Peru's continental shelf basins: Oil and Gas Journal, v. 96/46, p. 92-96.

Zúñiga y Rivero, F.J, J.A. Keeling, and H. Hay-Roe, 1998d, New hunting grounds studied on Peru's continental slope: Oil and Gas Journal, v. 96/49, p. 87-92.

Zúñiga y Rivero, F.J., H. Hay-Roe, and T. Vargas, 1999, Untested potential under 50 million acres in offshore Peru: Oil and Gas Journal, v. 96/11, p. 67-72.

Zúñiga y Rivero, F.J., G.D. Klein, H. Hay-Roe, and E. Álvarez-Calderon, 2010, The hydrocarbon potential of Peru: Lima, Peru: BPZ Exploración & Producción S.R.L., 338 p.